

ORIGINAL RESEARCH ARTICLE

# Extracellular Vesicles From Epicardial Fat Facilitate Atrial Fibrillation

Olga Shaihov-Teper, MSc\*; Eilon Ram<sup>1</sup>, MD\*; Nimer Ballan, MSc; Rafael Y. Brzezinski<sup>1</sup>, MSc; Nili Naftali-Shani, PhD; Rula Masoud, PhD; Tamar Ziv, PhD; Nir Lewis, MSc; Yeshai Schary, MSc; La-Paz Levin-Kotler, PhD; David Volvovitch, MD; Elchanan M. Zuroff, MD; Sergei Amunts, MD; Neta Regev-Rudzki<sup>1</sup>, PhD; Leonid Sternik, MD; Ehud Raanani, MD; Lior Gepstein, MD, PhD; Jonathan Leor<sup>1</sup>, MD

**BACKGROUND:** The role of epicardial fat (eFat)-derived extracellular vesicles (EVs) in the pathogenesis of atrial fibrillation (AF) has never been studied. We tested the hypothesis that eFat-EVs transmit proinflammatory, profibrotic, and proarrhythmic molecules that induce atrial myopathy and fibrillation.

**METHODS:** We collected eFat specimens from patients with (n=32) and without AF (n=30) during elective heart surgery. eFat samples were grown as organ cultures, and the culture medium was collected every 2 days. We then isolated and purified eFat-EVs from the culture medium, and analyzed the EV number, size, morphology, specific markers, encapsulated cytokines, proteome, and microRNAs. Next, we evaluated the biological effects of unpurified and purified EVs on atrial mesenchymal stromal cells and endothelial cells in vitro. To establish a causal association between eFat-EVs and vulnerability to AF, we modeled AF in vitro using induced pluripotent stem cell-derived cardiomyocytes.

**RESULTS:** Microscopic examination revealed excessive inflammation, fibrosis, and apoptosis in fresh and cultured eFat tissues. Cultured explants from patients with AF secreted more EVs and harbored greater amounts of proinflammatory and profibrotic cytokines, and profibrotic microRNA, as well, than those without AF. The proteomic analysis confirmed the distinctive profile of purified eFat-EVs from patients with AF. In vitro, purified and unpurified eFat-EVs from patients with AF had a greater effect on proliferation and migration of human mesenchymal stromal cells and endothelial cells, compared with eFat-EVs from patients without AF. Last, whereas eFat-EVs from patients with and without AF shortened the action potential duration of induced pluripotent stem cell-derived cardiomyocytes, only eFat-EVs from patients with AF induced sustained reentry (rotor) in induced pluripotent stem cell-derived cardiomyocytes.

**CONCLUSIONS:** We show, for the first time, a distinctive proinflammatory, profibrotic, and proarrhythmic signature of eFat-EVs from patients with AF. Our findings uncover another pathway by which eFat promotes the development of atrial myopathy and fibrillation.

**Key Words:** angiotensin-converting enzyme 2 ■ atrial fibrillation ■ exosomes ■ extracellular vesicles ■ fibrosis ■ inflammation

**A**trial fibrillation (AF) is a global epidemic with significant morbidity, mortality, and socioeconomic burden.<sup>1–3</sup> A major predisposing factor to the initiation and sustention of AF is atrial myopathy. It results from hemodynamic or metabolic stresses that stimulate fibrosis, remodeling, electric abnormalities, and rheological dysfunction in the atria.<sup>4–6</sup> AF itself exacerbates many of these

features, which explains its progressive nature.<sup>4–6</sup> Today, an upstream treatment for atrial myopathy is lacking.

Obesity is a major modifiable risk factor for AF.<sup>7</sup> The mechanism is complex and not entirely clear, but it may be mediated by abnormal deposition of epicardial fat (eFat).<sup>8–10</sup> Abnormal eFat is a source of proinflammatory and fibrotic molecules that can affect the adjacent atria,

Correspondence to: Jonathan Leor, MD, FACC, Neufeld Cardiac Research Institute, Sheba Medical Center, Tel-Hashomer 52621, Israel. Email leorj@post.tau.ac.il  
\*O. Shaihov-Teper and E. Ram contributed equally.

The Data Supplement is available with this article at <https://www.ahajournals.org/doi/suppl/10.1161/CIRCULATIONAHA.120.052009>.  
For Sources of Funding and Disclosures, see page 2491.

© 2021 American Heart Association, Inc.  
Circulation is available at [www.ahajournals.org/journal/circ](http://www.ahajournals.org/journal/circ)

## Clinical Perspective

### What Is New?

- The present study is the first to examine the role of epicardial fat–derived extracellular vesicles (eFat-EVs) in the pathogenesis of atrial fibrillation (AF).
- We found another pathway that links eFat to AF.
- We show that eFat-EVs of patients with AF have unique proinflammatory, profibrotic, and proarrhythmic properties.
- eFat-EVs can induce cellular, molecular, and electrophysiological remodeling that can result in atrial fibrosis, myopathy, and the development of AF.

### What Are the Clinical Implications?

- Understanding of the role of eFat-EVs in the pathogenesis of AF may lead to the discovery of new diagnostic markers and novel targets for the prevention and treatment of AF.
- The proinflammatory, profibrotic, and proarrhythmic effects of eFat-EVs may be relevant to the pathogenesis of other cardiovascular diseases associated with obesity and abnormal adipose tissue deposition.

induce atrial myopathy, and generate the arrhythmogenic substrate needed to initiate and sustain AF.<sup>10–13</sup>

Proinflammatory and fibrotic molecules can be secreted while encapsulated within extracellular vesicles (EVs).<sup>14,15</sup> These EVs are membrane-bound organelles that are extruded from all cell types, traffic to local or distant targets, and execute biological functions.<sup>14,15</sup> EVs carry proteins, nucleic acids, and lipids that transmit the molecular signature of the cells of origin. Adipose tissue–derived EVs have been implicated in obesity-related diseases such as metabolic syndrome, type 2 diabetes, and endothelial dysfunction.<sup>16</sup> However, the role of eFat-EVs in the pathogenesis of AF has never been studied. Here, we hypothesized that eFat causes atrial myopathy and fibrillation by releasing EVs that carry proinflammatory, profibrotic, proarrhythmic molecules to the atria. Revealing this pathway in the pathogenesis of AF may identify new risk markers and therapeutic targets to prevent and treat AF and associated complications.

## METHODS

A detailed description of the methods is provided in the [Data Supplement Materials](#). All data that support the findings are available within the article and in the [Data Supplement](#), and are available on reasonable request, as well.

### Patients

The study was approved by an institutional review board of Sheba Medical Center and Tel Aviv University. The participants gave written informed consent. Cardiac eFat specimens were collected from patients with and without AF undergoing

## Nonstandard Abbreviations and Acronyms

<b>AF</b>	atrial fibrillation
<b>APD</b>	action potential duration
<b>APD<sub>80</sub></b>	action potential duration at 80% repolarization
<b>ECs</b>	endothelial cells
<b>eFat</b>	epicardial Fat
<b>EGF</b>	epidermal growth factor
<b>EVs</b>	extracellular vesicles
<b>FGF</b>	fibroblast growth factor
<b>hiPSC</b>	human induced pluripotent stem cells
<b>hiPSC-CCS</b>	human induced pluripotent stem cells - cardiac cell sheets
<b>IL</b>	Interleukin
<b>miRNA</b>	microRNA
<b>MS</b>	mass spectrometry
<b>MSCs</b>	mesenchymal stromal cells
<b>NTA</b>	nanoparticle tracking analysis
<b>PANTHER</b>	protein analysis through evolutionary relationships
<b>SEC</b>	size exclusion chromatography
<b>sFLT-1</b>	soluble fms-like tyrosine kinase-1
<b>TGF-<math>\beta</math></b>	transforming growth factor $\beta$
<b>TIMP-4</b>	tissue inhibitor of matrix metalloproteinase
<b>TNF-<math>\alpha</math></b>	tumor necrosis factor – $\alpha$
<b>TSG101</b>	tumor susceptibility gene 101
<b>UC</b>	ultracentrifugation
<b>VEGF</b>	vascular endothelial growth factor

elective open heart surgery. We diagnosed AF based on the patient's medical history and hospital records before the surgery. Classification to AF was based on the American Heart Association/American College of Cardiology definition.<sup>17</sup>

### eFat Biopsy and Organ Culture

The site of biopsy was the eFat near the base of the pulmonary arteries. eFat specimens were cut into small pieces of 1 mm<sup>3</sup> and incubated as organ culture for 9 days. To isolate and purify EVs, medium was collected and renewed 2, 4, 6, and 9 days after organ culture.

### eFat Histology

We examined fresh and cultured (day 9) eFat specimens. To assess cell viability in vitro, we used a 2,3-bis-(2-methoxy-4-nitro-5-sulphophenyl)-2H-tetrazolium-5-carboxanilide salt–based colorimetric assay.

### Isolation, Separation, and Purification of eFat-EVs

Our methods for isolating eFat-EVs were guided by the recent position statement of the International Society for Extracellular

Vesicles (MIEV2018).<sup>18</sup> The information about EV isolation and separation has been uploaded to the EV-TRACK knowledge-base. Readers may access the experimental parameters in the following URL: <http://evtrack.org/review.php> (EV-TRACK ID: EV190048, Shaihov-Teper).

### Nanoparticle Tracking Analysis

The amount and size distribution of isolated EVs were examined by conducting nanoparticle tracking analysis (NTA), using the Malvern NanoSight NS300 (Malvern) device.

### Electron Microscope

eFat-EVs of patients with and without AF were loaded onto formvar carbon-coated grids, then fixed, washed, and examined in a JEM-1400Plus Transmission Electron Microscope (JEOL).

### Protein Content

Isolated EVs were treated with radioimmunoprecipitation assay buffer (Thermo-Fisher Scientific). Protein content of isolated EVs was measured by using BCA Pierce Protein Assay Kit (Thermo-Fisher Scientific).

### High-Density Lipoprotein and Low-Density Lipoprotein/Very-Low-Density Lipoprotein

High-density lipoprotein and low-density lipoprotein/very-low-density lipoprotein levels in size exclusion chromatography (SEC)-purified EV fractions were quantified by lipoprotein kit (Abcam ab65390).

### EV-Associated Markers by Western Blot

Markers for eFat-EVs were analyzed by Western blot and were probed for the EV-associated markers CD63, CD81, and TSG101 (Santa Cruz Biotechnology).

### EV Characterization by Flow Cytometry

EV-coated beads were resuspended with phosphate-buffered saline and analyzed by flow cytometry using a flow-activated cell sorter Calibur flow cytometer (Cyteck Development) and FlowJo software (Tree Star).

### Cytokine Array and Enzyme-Linked Immunosorbent Assay

To expose EV protein content, isolated EVs were treated with radioimmunoprecipitation assay buffer. Free and EV-encapsulated cytokines were quantified by Q-Plex Human Custom (4-plex) array (Quansys Biosciences) or commercially available kits of sandwich enzyme-linked immunosorbent assay (Biolegend).

### Mass Spectrometry–Based Proteomic Analysis

Samples of eFat-EVs, isolated by either ultracentrifugation (UC) or SEC were analyzed by a Q-Exactive plus mass spectrometer (QE, Thermo).<sup>19</sup> The mass spectrometry proteomics data have been deposited in the ProteomeXchange Consortium through the PRIDE partner repository.

### miRNA Extraction and Analysis

Total microRNA (miRNA) was extracted from the purified EVs using a total EV RNA and Protein Isolation kit (Invitrogen).

### Migration Scratch Assay

To determine the effect of eFat-EVs on atrial mesenchymal stromal cells (MSCs), we used human MSCs, isolated from human right atrial appendage, and a migration (scratch) assay.

### EV Uptake by Human Endothelial Cells

eFat-EVs were labeled with PKH26 (red fluorescent cell linker kits for general cell membrane labeling) and incubated with human umbilical cord vascular endothelial cells in a special chamber using the LSM 700 confocal microscope (ZEISS) with incubator-like conditions and video recording.

### Angiogenic Tube Formation Assay

We used the human umbilical cord vascular endothelial cell Matrigel tube formation assay. Microscopic pictures of each well, and the amount and structure of the tubes were captured and evaluated after 11 hours.

### Generation and Optical Mapping of a Human Induced Pluripotent Stem Cell–Derived Cardiac Cell Sheet

To demonstrate the causal association of eFat-EVs and vulnerability to arrhythmias, we used a transgenic human-induced pluripotent stem cells (hiPSC) line that stably expresses ArcLight.<sup>20</sup> Optical mapping was performed in a hiPSC-based cardiac cell sheet (hiPSC-CCS) tissue model derived from the ArcLight-expressing hiPSC cardiomyocytes.<sup>20</sup> From the optically derived action potentials, we constructed detailed activation maps enabling measurements of electrophysiological parameters related to conduction velocity and repolarization ( $APD_{80}$ , action potential duration at 80% of repolarization) at several time points during the experiment.<sup>20</sup> Arrhythmia inducibility in the culture was evaluated at 168 hours, using a 3-step programmed electric stimulation protocol.<sup>20</sup>

### Injection of EVs into Rat Hearts

Animal experiments were performed in accordance with the Guide for the Care and Use of Laboratory Animals and were approved by the Institutional Animal Care and Use Committee of the Sheba Medical Center. To assess the in vivo profibrotic effects of eFat-EVs, we injected eFat-EVs into the left ventricular anterior wall of the rats. The rats received 2 injections of 50  $\mu$ L unpurified eFat-EVs ( $6 \times 10^8$  EVs each, total 10  $\mu$ g/100  $\mu$ L) from patients either with or without AF. Hearts were harvested for histological analysis 7 days after the injections.

### Statistical Analysis

Demographic and clinical data are expressed as mean  $\pm$  SD. Experimental data are expressed as mean  $\pm$  SEM. Specific statistical tests are detailed in the figure legends and the [Data Supplement Methods](#).

## RESULTS

### Patient Characteristics

We collected eFat specimens from 62 patients with heart disease, with and without AF, who underwent elective open heart surgery (Table). Most of the demo-

graphic, clinical characteristics, treatments, and indications for surgery were similar for patients with and without AF (Table). Previous heart surgery was more frequent among patients with AF. The prevalence of risk factors for AF, such as obesity, hypertension, and diabetes were similar. The mean left atrial size, pulmonary

**Table. Patient Characteristics.**

Characteristics	AF (n=32)	No-AF (n=30)	P value
Age, y, mean±SD	69±11	63±13	0.06
Sex, male (%)	18 (56)	18 (60)	0.8
Paroxysmal AF (%)	13 (41)	0(0)	<0.001
Previous heart surgery (%)	6 (19)	0 (0)	0.02
Hypertension (%)	22 (69)	19 (63)	0.79
Body mass index, kg/m <sup>2</sup> , mean±SD	26.1±3.3	28.1±3.9	0.12
Obesity (%)	6 (19)	12 (40)	0.09
Diabetes (%)	14 (44)	10 (33)	0.44
Insulin (%)	2 (6)	6 (20)	0.14
Noninsulin-dependent diabetes (%)	12 (37)	4 (13)	0.04
Ischemic heart disease (%)	16 (50)	17 (57)	0.62
Heart failure with preserved ejection fraction (%)	0 (0)	0 (0)	1.0
Renal impairment (%)	9 (28)	6 (20)	0.56
Chronic obstructive pulmonary disease (%)	3 (9)	3 (10)	1.0
Obstructive sleep apnea (%)	2 (6)	0 (0)	0.49
Dyslipidemia (%)	21 (66)	23 (77)	0.41
Peripheral vascular disease (%)	4 (12)	2 (7)	0.67
Medication			
Anticoagulation (%)	29 (91)	3 (10)	<0.001
Statin therapy (%)	21 (66)	21 (70)	0.79
Echocardiographic			
Left ventricular ejection fraction, %, mean±SD	53.8±11.1	57.1±10.9	0.05
Left ventricular end diastolic diameter, mean±SD	50.1±7.6	47.8±6.8	0.27
Left atrium diameter anteroposterior, mm, mean±SD	50.3±8.7	37.9±5.9	<0.001
Left atrium systolic area, cm <sup>2</sup> , mean±SD	35.1±11.8	21.4±6	<0.001
Moderate/severe mitral regurgitation (%)	15 (47)	12 (41)	0.79
Moderate/ severe mitral stenosis (%)	8 (25)	3 (10)	0.19
Moderate/ severe aortic stenosis (%)	7 (22)	7 (24)	1.0
Moderate/ severe tricuspid regurgitation (%)	9 (28)	4 (14)	0.22
Systolic pulmonary artery pressure, mean±SD	48.2±18.8	37.8±14	0.02
Surgery			
Mitral valve repair/replacement (%)	22 (69)	13 (43)	0.07
Aortic valve replacement (%)	9 (28)	9 (30)	1.0
Tricuspid valve repair (%)	11 (34)	3 (10)	0.03
Coronary artery bypass grafting (%)	11 (34)	14 (47)	0.44
Maze procedure (%)	8 (25)	0 (0)	0.01

Classification to atrial fibrillation (AF) was based on the American Heart Association/American College of Cardiology Definition: Paroxysmal AF was defined as episodes of AF that terminated spontaneously within 7 days. Chronic AF included persistent AF (episodes of AF that lasted for >7 days and required pharmacological or electric intervention to terminate), long-standing persistent AF (AF that has persisted for >12 months, either because cardioversion had failed or because cardioversion had not been attempted), and permanent AF.<sup>17</sup> The statistical method used was Fisher exact test for comparison of categorical variables, and a Mann-Whitney *U* test for comparison of continuous variables.

pressure, use of anticoagulants, and need for tricuspid repair or Maze procedure were all greater in patients with AF (Table). Overall, the characteristics of patients enrolled in our study were representative of patients referred for elective heart surgery.

To further characterize patients with AF, we conducted a subgroup analysis of the first 27 patients with paroxysmal AF versus chronic AF (persistent, long-standing persistent, or permanent AF). We observed that the frequency of ischemic heart disease and coronary artery bypass graft surgery was higher in patients with paroxysmal AF (Table I in the Data Supplement).

### Excessive Inflammation and Fibrosis in eFat From Patients With Heart Disease

To characterize the eFat specimens, we examined fresh and cultured (9 days) eFat explants. Histological analysis revealed extensive inflammation and fibrosis in eFat from fresh and cultured explants from patients with and without AF (Figure 1). Microscopic examination revealed regions with distortion of the typically homogeneous and finely divided faint septa with excessive extracellular matrix deposition (Figure 1A), thick bands of collagen and extensive fibrosis (Figure 1B), clusters of macrophages (Figure 1C), myofibroblasts (Figure 1D), endothelial cells (ECs; Figure 1E), and apoptotic cells (Figure 1F).

Another new finding was a robust expression of angiotensin-converting enzyme 2 at the sites of extracellular matrix thickening in fresh eFat from patients with and without AF (Figure 1G and 1H). This finding may explain the vulnerability of obese patients to coronavirus disease 2019 (COVID-19) complications, given that angiotensin-converting enzyme 2 mediates the entry of severe acute respiratory syndrome coronavirus 2 (SARS-CoV-2) into cells.<sup>21</sup>

Next, we assessed changes in cell viability in the eFat explants (n=2) by 2,3-bis-(2-methoxy-4-nitro-5-sulfophenyl)-2*H*-tetrazolium-5-carboxanilide salt-based colorimetric assay. Cell viability was unchanged throughout 9 days (Figure 1I), suggesting that the growth and death of cells in the cultured explant remained balanced. Cell activity was greater in eFat from patients with AF than those without AF (Figure 1I). The eFat from all patients referred for open heart surgery was collectively characterized by unresolved chronic inflammation, cell death, fibrosis, and angiogenesis.

### eFat From Patients With AF Secreted EVs With a Distinctive Profile

EVs carry molecules that transmit the molecular signature of their originating cells.<sup>14,15,22</sup> To determine the profile of eFat-EVs from patients with AF, we tested several methods to isolate EVs from the culture medium of eFat explants and compared the results of these methods. UC

is the most commonly used method for isolating EVs,<sup>23</sup> so we used UC on 1 group of eFat samples (n=39) from patients with AF (n=20) and without AF (n=19). On a second group of eFat samples (n=10), we used SEC to improve EV purity and to reduce contaminants. We then compared the characteristics, cargo, and biological functions of EVs isolated by SEC versus UC. Last, for the electrophysiological studies, we isolated and separated eFat-EVs by 30% density sucrose cushion (n=13).

First, we used UC to isolate eFat-EVs. We analyzed the amount and size of EVs by NTA (Figure 2A) and found that most EVs were in the range of 50 to 250 nm (Figure 2B). eFat specimens from patients with AF secreted more EVs than did specimens from patients without AF (Figure 2B). eFat of patients with chronic AF secreted greater amounts of EVs than patients with paroxysmal AF or without AF (Figure 2C), suggesting higher biological activity in eFat from patients with chronic AF. Next, we confirmed the EV phenotype by transmission electron microscopy (Figure 2D) and immunoblotting by Western blot probed for EV (CD63, CD81) and exosome (TSG101) associated markers (Santa Cruz Biotechnology; Figure 2E).<sup>18</sup>

To characterize the content of eFat-derived EVs, we performed a cytokine array that identified certain proteins plausibly related to the pathogenesis of atrial myopathy and fibrillation. Isolated EVs were treated with radioimmunoprecipitation assay buffer (Thermo-Fisher Scientific) to expose their protein content. We analyzed both EV-encapsulated (Figure 2F–2M) and free soluble cytokines (Figure 2N–2U) in the medium of eFat explants. Cytokine analysis revealed that eFat-EVs from patients with AF harbored higher amounts of proinflammatory and profibrotic cytokines, and adiponectin, as well, than patients without AF. These encapsulated cytokines, such as IL-1 $\alpha$  (interleukin 1 $\alpha$ ), IL-6 (interleukin 6), TNF- $\alpha$  (tumor necrosis factor  $\alpha$ ), IL-4 (interleukin 4; Figure 2F–2I) have been implicated in the pathogenesis of AF.<sup>24</sup> eFat-EVs from patients with AF had lower levels of IL-10 (interleukin 10; an anti-inflammatory profibrotic cytokine; Figure 2J), VEGF (vascular endothelial growth factor; Figure 2L), and soluble VEGF receptor (sFLT-1 [soluble fms-like tyrosine kinase-1]; Figure 2M), than patients without AF.

In parallel, analysis of free soluble cytokines (Figure 2N–2U) from the culture medium revealed that, excluding IL-1 $\alpha$ , the differences in cytokine levels between patients with and without AF disappeared. Furthermore, except for IL-1 $\alpha$ , there was no correlation between the amount of eFat-derived free (soluble) cytokines and cytokines encapsulated in EVs (Figure 2V). Together, our findings indicated that eFat-EVs carried a unique profile of proinflammatory and profibrotic cytokines. Compared with free cytokines, the cargo of eFat-EVs better differentiated between patients with AF versus patients without AF.

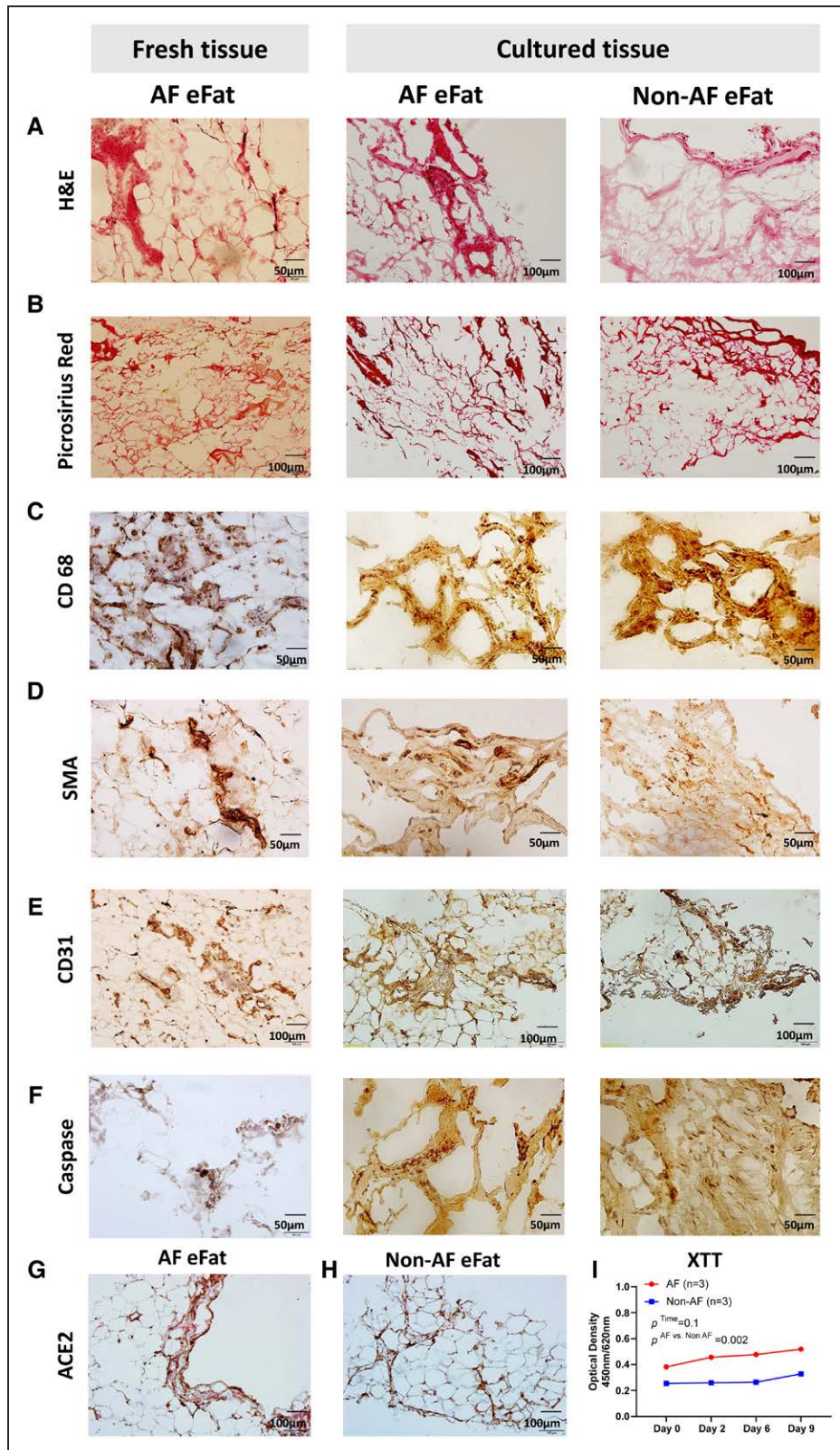


**Figure 1. Extensive inflammation and fibrosis in eFat of patients with and without AF.**

To characterize the eFat from cardiac patients, we obtained eFat from patients with and without AF. The site of biopsy was the eFat near the base of the pulmonary arteries. Fresh and cultured eFat were cryosectioned and stained with: **A**, H&E. **B**, Picrosirius red for collagen and fibrosis. **C**, Anti-CD68 antibodies for macrophages. **D**, Anti-SMA antibodies for myofibroblasts, smooth muscle cells, and pericytes. **E**, Anti-CD31 antibodies for endothelial cells. **F**, Anti-caspase antibodies for apoptotic cells. **G** and **H**, Anti-ACE2 antibodies. Microscopic examination of eFat specimen revealed distortion of the typically homogeneous and finely divided faint septa with excessive extracellular matrix deposition (**A**), (Continued)

**Figure 1 Continued.** thick bands of collagen and extensive fibrosis (**B**), clusters of macrophages (**C**), myofibroblasts (**D**), endothelial cells (**E**), apoptotic cells (**F**), and robust expression of ACE2 at the regions of inflammation and fibrosis (**G** and **H**;  $n=2$ ; scale bars, 50–100  $\mu\text{m}$ ). **I**, XTT-based colorimetric assay of cultured eFat explant from patients ( $n=2$ ) with and without AF revealed a relatively constant number of viable cells in the eFat explant over 9 days (experiments were performed in triplicates). *P* values by repeated-measures 2-way ANOVA and the Sidak post test. ACE2 indicates angiotensin-converting enzyme 2; AF, atrial fibrillation; eFat, epicardial fat; H&E, hematoxylin-eosin; SMA, smooth muscle actin; and XTT, 2,3-bis-(2-methoxy-4-nitro-5-sulfophenyl)-2*H*-tetrazolium-5-carboxanilide salt.

## EV Purification Preserved the Distinct Profile of eFat-EVs From Patients With AF

Isolation of EVs by UC may cause nonvesicular macromolecule contamination that can lead to decreased sample purity and may affect downstream analysis.<sup>18</sup> To determine the relative contribution of pure EVs versus EVs with contaminated proteins, we purified and enriched EVs by SEC,<sup>25</sup> which emerged as a reliable and efficient method to improve EV isolation, eliminate protein contamination, and preserve the biological properties of isolated EVs, all with high reproducibility.<sup>25</sup> The samples ( $n=10$ ) were allowed to run into the column, and the eluate was collected into 36 sequential fractions of 2 mL (Figure 3A). Then, using NTA, we analyzed the concentration of particles, proteins, and lipoproteins in each fraction. NTA showed that the particles were eluted in fractions 2 to 18 and fractions 19 to 25. Protein analysis of each fraction revealed clusters of protein in fractions 26 to 36 (Figure 3A). The pattern of size distribution in SEC fractions (Figure 3B) indicated a greater amount and larger size of particles in fractions 1 to 18 than in 19 to 25 (Figure 3A and 3B). The unusual pattern of 2 peaks of EVs over various SEC fractions (Figure 3A) is probably related to the heterogeneous EV sources in the eFat explant, compared with a homogeneous single-cell culture or serum.

Additional NTA comparison from fractions 2 to 18 revealed that most of the EVs were in the range of 50 to 150 nm, with diverse size distribution between EVs derived from patients with versus patients without AF (Figure 3C). Thus, the SEC-based purified eFat-EVs were compatible with the definition of small EVs.<sup>18</sup>

Particles detected by NTA are not necessarily EVs, but may also be protein aggregates and lipoproteins.<sup>26</sup> We detected pure EVs in the SEC eluate fractions 2 to 18, according to transmission electron microscopy (Figure 3D) and their positivity for the EV protein CD81, with >60% purity (Figure 3E and 3F). Fractions 19 to 25 were contaminated by proteins (Figure 3A) and contained higher amounts of very-low-density lipoprotein, low-density lipoprotein, and high-density lipoprotein (Figure 3G and 3H). We thus focused on EV-rich, protein low eluate fractions (2–18).

To determine whether SEC-based EV purification affects the signature of eFat-EVs, we reanalyzed several representative cytokines in purified (SEC, upper graphs) and unpurified (UC, lower graphs) eFat-EVs (Figure 3I–3N). Both purified and unpurified eFat-EVs from patients with AF carried a greater amount of proinflammatory

cytokines such as IL-1 $\alpha$  and IL-6, profibrotic cytokines such as osteopontin, a mediator of cardiac aging, atherosclerosis, and fibrosis,<sup>27</sup> and the protective adipokine adiponectin, as well (Figure 3I–3L). The amounts of the EV-encapsulated cytokines TNF $\alpha$  and IL-1 $\beta$  were similar in patients with and without AF. Collectively, the unique profile of eFat-EVs from patients with AF was preserved after EV purification.

## Distinct Proteomic Profile of eFat-EVs From Patients With AF

Proteomic analysis provides systematic high-throughput analysis of proteins and holds the promise for the discovery of novel biomarkers and therapeutic targets. To better determine the distinctive profile of eFat-EVs from patients with AF and explore differences in the proteome of eFat-EVs from patients with versus without AF, we performed comparative proteomic profiling.

To further identify potential candidate protein components from the EV cargo that may be responsible for the observed fibrosis, angiogenesis, and reentry arrhythmias, we used mass spectrometry (MS) proteomics on eFat-EVs, isolated by UC or SEC, from patients with and without AF (Figure 4). First, we analyzed EVs separated by UC. We identified a greater abundance of proteins in the unpurified EVs from patients without AF (Figure 4A). Of the 581 quantified proteins, we identified 206 (35.5%) with a higher abundance in the AF samples and 375 (64.5%) with a higher abundance in the non-AF samples (Figure 4A). All identified proteins were clustered according to the PANTHER (Protein Analysis Through Evolutionary Relationships) classification system to various categories, including PANTHER pathways (Figure 4B), biological processes (Figure 4A in the Data Supplement), cellular component (Figure 4B in the Data Supplement), protein class (Figure 4C in the Data Supplement), and molecular function (Figure 4D in the Data Supplement). Analysis of various pathways indicated that EV-packaged proteins from the eFat of patients with AF and without AF have distinct proteomic profiles. For example, the PANTHER classification system revealed pathways relevant to fibrosis, angiogenesis, and coagulation in EVs from patients both with and without AF (Figure 4B). These proteins tended to be more abundant in EVs from patients without AF (Figure 4B). However, specific pathways related to fibrosis and hypertrophy, such as TGF- $\beta$  (transforming growth factor  $\beta$ ) and 5-hydroxytryptamine pathways, were exclusively expressed in eFat-EVs from patients with AF.

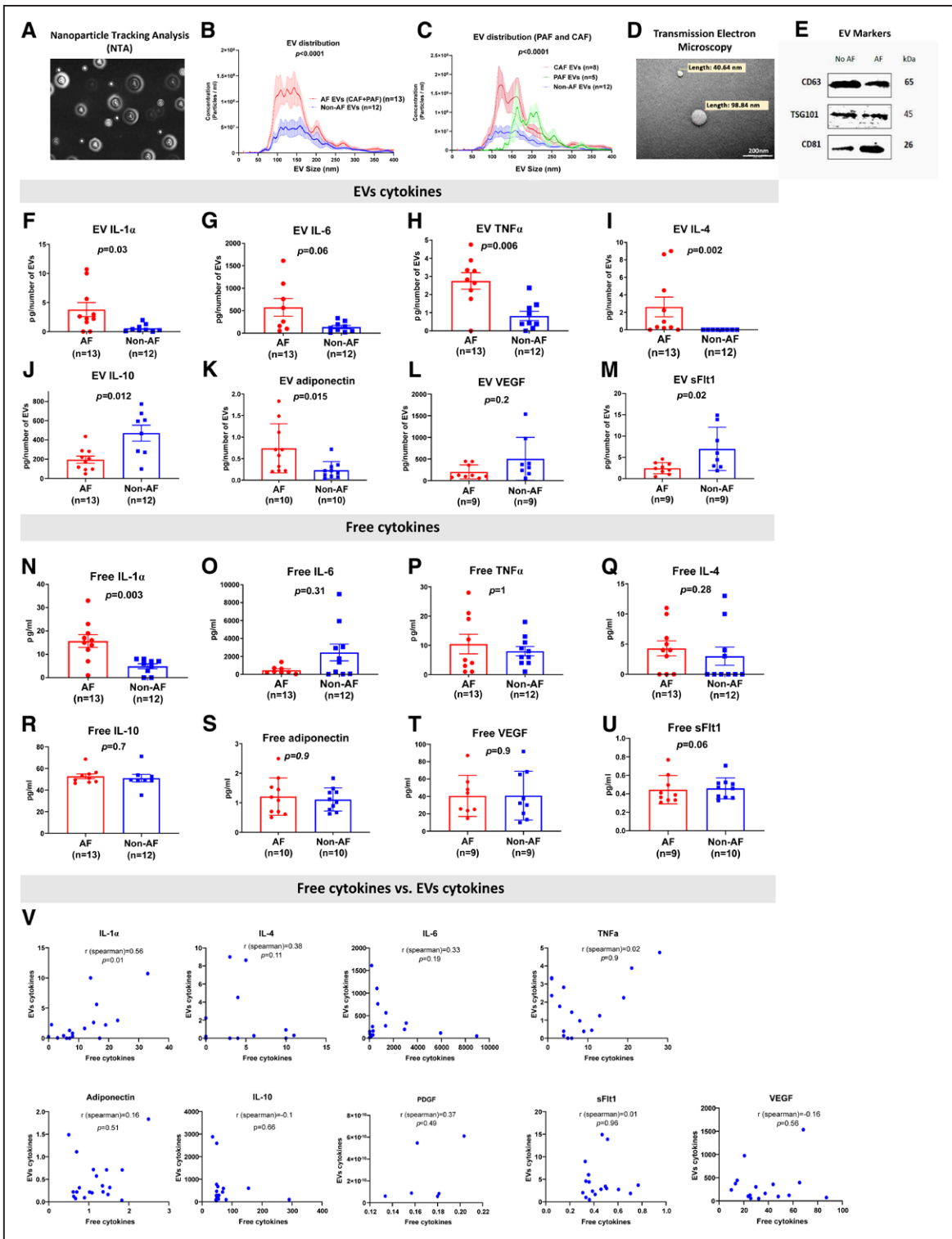


**Figure 2. Characterization of unpurified eFat-EVs from patients with and without AF.**

To characterize the eFat-EVs, we cut eFat specimens into small pieces of 1 mm<sup>3</sup> and incubated the explants in serum-free culture for 9 days. To isolate EVs, the culture medium was collected and renewed every 2, 4, 6, and 9 days. eFat-EVs were isolated by ultracentrifugation. Size, distribution, and concentration of EVs were evaluated by NTA. **A**, Representative NTA image of eFat-EVs from patients with and without AF. **B**, Size distribution and concentration analysis of eFat-EVs revealed a higher concentration of eFat-EVs secreted from patients with AF (CAF and PAF) than those without AF ( $P < 0.0001$  by Kolmogorov-Smirnov test). **C**, Subgroup analysis showed a higher concentration of eFat-EVs from patient with CAF than those with PAF or without AF ( $P < 0.0001$  by Kolmogorov-Smirnov test). **D**, Representative transmission electron microscopy image of eFat-EVs from patients with AF (scale bar, 200 nm). **E**, Representative Western immunoblot confirmed the presence of the EV-associated markers CD63, TSG101, and CD81 (n=3). **F** through **M**, To determine the content of eFat-EVs, we measured and compared the levels of EV-encapsulated cytokines and free cytokines from patients with and without AF. (Continued)

**Figure 2 Continued.** Cytokine analysis revealed that eFat-EVs from patients with AF carried higher amounts of proinflammatory and profibrotic cytokines IL-1 $\alpha$  (**F**), IL-6 (**G**), TNF- $\alpha$  (**H**), IL-4 (**I**), and adiponectin (**K**), as well, but lower amounts of IL-10 (**J**), VEGF (**L**), and sFLT-1 (**M**) than patients without AF. **N** through **U**, Excluding IL-1 $\alpha$ , the levels of soluble free cytokines secreted from eFat explants were similar in patients with and without AF ( $n=25$ , results are presented as the mean of cytokine secretion levels [pg/number of EVs $\pm$ SEM] for EV-encapsulated cytokines and [pg/mL $\pm$ SEM] for free cytokines,  $P$  values were calculated by the Mann-Whitney  $U$  test). **V**, Except for IL-1 $\alpha$ , there was no correlation between the amount of eFat-derived free (soluble) cytokines (**N** through **U**) and the cytokines encapsulated in EVs ( $n=12$ ,  $P$  values were calculated by Spearman correlation test). AF indicates atrial fibrillation; CAF, chronic atrial fibrillation; eFat, epicardial Fat; EVs, extracellular vesicles; IL, interleukin; NTA, nanoparticle-tracking analysis; PAF, paroxysmal atrial fibrillation; sFLT-1, soluble fms-like tyrosine kinase-1; TNF- $\alpha$ , tumor necrosis factor- $\alpha$ ; TSG101, tumor susceptibility gene 101; and VEGF, vascular endothelial growth factor.

Subgroup classification of the 16 proteins with difference of  $P<0.05$  (Table II in the Data Supplement) confirmed the distinct profile of EVs from patients with and without AF (Figure II in the Data Supplement).

Contaminants of the unpurified EV samples may mask the signal of lower abundant EV proteins and interfere with the MS data analysis. To exclude the effect of contaminated proteins on the interpretation of MS data, we repeated the MS analysis with purified EVs by SEC and confirmed the elimination of many proteins (Figure 4C). The distinctive proteomic profile of eFat-EV-encapsulated proteins from patients with AF was more prominent in purified eFat-EVs. Of the 371 quantified proteins, we identified 259 (70%) with a higher abundance in the eFat-EVs from patients with AF, and 112 (30%) with higher abundance in the eFat-EV sample from patients without AF (Figure 4C).

The PANTHER classification system revealed that several pathways related to atrial fibrosis, angiogenesis, apoptosis, and myopathy were exclusively expressed in purified eFat-EVs from patients with AF (Figure 4D). These pathways include wntless and Int-1 pathway signaling, 5-hydroxytryptamine pathways, T-cell activation, VEGF, FGF (fibroblast growth factor), and EGF (epidermal growth factor) signaling (Figure 4D). Further classification to various categories, including biological processes (Figure IIIA in the Data Supplement), cellular component (Figure IIIB in the Data Supplement), protein class (Figure IIIC in the Data Supplement), and molecular function (Figure IIID in the Data Supplement) confirmed the unique proteomic profile of eFat-EVs from patients with AF. Overall, eFat-EVs from patients with AF secreted a distinct proteomic signature enriched in cytoskeletal regulation, inflammatory, fibrotic, and angiogenic proteins. In addition, metabolic changes were observed as elevation in glycolytic enzymes and other ATP synthesis proteins, as well, in patients with AF. Subgroup classification of the 22 proteins with difference of  $P<0.05$  (Table II in the Data Supplement) confirmed the distinct profile of EVs from patients with AF (Figure IV in the Data Supplement).

### eFat-EVs Stimulated Fibrosis

Atrial fibrosis plays a significant role in the pathogenesis of AF.<sup>12,13,28,29</sup> To demonstrate a causal association between eFat-EVs and atrial fibrosis, we used a scratch

migration (wound-healing) assay with human right atrial MSCs.<sup>30</sup> We found that eFat-EVs from patients with AF stimulated MSC migration and gap closure faster than patients without AF (Figure 5A and 5B).

To exclude the potential effect of contaminated proteins on the profibrotic effects of eFat-EVs, we repeated the scratch assay after EV purification by SEC. EV rich, protein low fractions (1–18) were pooled and concentrated by UC to 700  $\mu$ L. Again, the profibrotic effect of eFat-EVs from patients with AF was significantly greater than in patients without AF, as indicated by the rate and magnitude of the gap closure within 48 hours (Figure 5C and 5D). The rate of the gap closure was slower in EVs isolated by SEC than by UC. Overall, the results of the functional assays after EV purification confirmed our initial findings that the eFat-EVs from patients with AF have profibrotic effects.

miRNAs have been linked to the pathogenesis of atrial remodeling and fibrillation. Although EVs facilitate transfer of miRNAs that regulate gene expression in recipient cells,<sup>31</sup> studies investigating the role of miRNAs in AF show conflicting results.<sup>32</sup> To determine the potential role of eFat EV-encapsulated miRNA, we measured several miRNAs that could influence cardiac fibrosis. miR-146b targets and inhibits TIMP-4 (tissue inhibitor of matrix metalloproteinase) and stimulates cardiac fibrosis. Expression of EV miR-146b was upregulated in eFat-EVs from patients with AF, compared with those without AF (Figure 5E). miR-133a targets and inhibits TGF- $\beta$ , decreases collagen content, and inhibits atrial remodeling. miRNA-29a suppresses collagen synthesis, and downregulation of miRNA-29a induces fibrosis.<sup>33</sup> Expression of EV miR-133a and 29a was downregulated in eFat-EVs from patients with AF, compared with those without AF (Figure 5F and 5G). Overall, eFat-EVs from patients with AF carried more profibrotic miRNAs than patients without AF.

Last, to confirm our findings in vivo, we injected eFat-EVs from patients with and without AF to the left ventricular anterior wall of 3 rats. Seven days later, we observed extensive myocardial fibrosis in the hearts treated with eFat-EVs from patients with AF (Figure 5H) compared with the heart treated with eFat-EVs from patients without AF (Figure 5I). Thus, our in vivo findings supported our in vitro data and indicated that eFat-EVs have profibrotic properties.

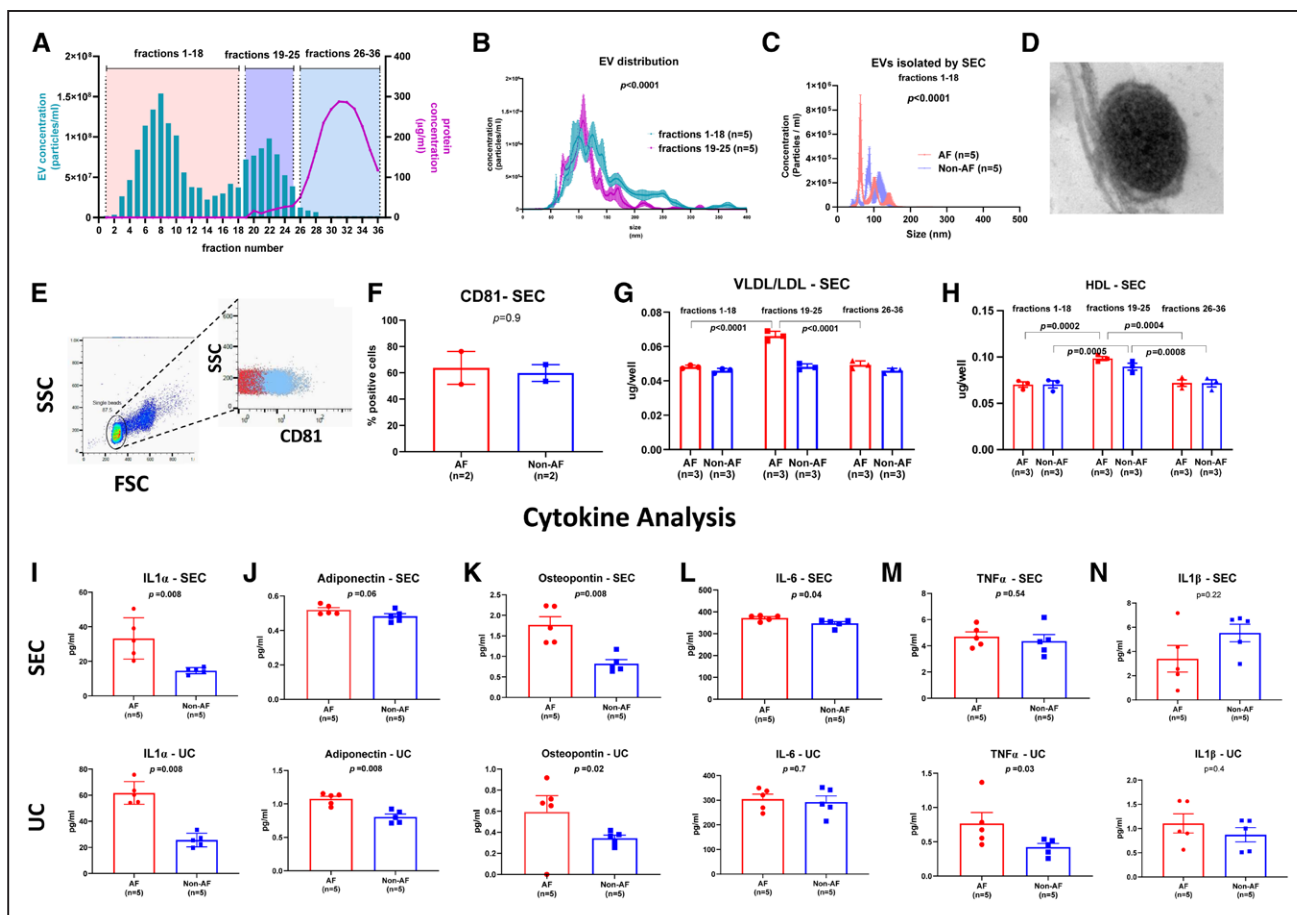


**Figure 3. Characterization of purified eFat-EVs from patients with and without AF.**

To further characterize eFat-EVs, we purified and enriched EVs by SEC. The eFat-EV samples were allowed to run into the column, and the eluate was collected into 36 sequential fractions of 2 mL. **A**, NTA and protein analysis revealed 2 peaks of particles (fractions 2–18 and 19–25), and late peak of protein (fractions 26–36;  $n=5$ , data shown as EV and protein concentration). **B**, NTA analysis revealed a greater number and larger size of particles in fractions 19 to 25 than 1 to 18 ( $P$  value was calculated by Kolmogorov-Smirnov test). **C**, NTA analysis of fractions 1 to 18 revealed EVs that ranged between 50 and 150 nm and varied between patients with and without AF ( $P$  values by Kolmogorov-Smirnov test). **D**, Representative transmission electron microscopy images of EVs from fractions 1 to 18 ( $n=5$ ; scale bar, 200 nm). **E**, Flow cytometry analysis of the EV marker CD81: FSC vs SSC dot plot where eFat-EVs are gated. Representative dot plot showing right shift of fluorescent intensity for the positive populations of beads: EVs complex (blue CD81+, red isotype;  $n=2$ ). **F**, eFat-EVs from patients with and without AF are >60% positive for CD81 ( $n=2$ , data are presented as % of positive cells,  $P$  values by Mann-Whitney  $U$  test). **G**, Analysis of the lipoproteins VLDL and LDL revealed higher amounts of lipoproteins in fractions 19 to 25 ( $n=5$ , data are presented as  $\mu\text{g}/\text{well}$  of lipoproteins,  $P$  values by 2-way ANOVA and Sidak post test). **H**, HDL analysis revealed higher amounts of lipoproteins in fractions 19 to 25 ( $n=5$ , data are presented as  $\mu\text{g}/\text{well}$  of lipoproteins,  $P$  values by 2-way ANOVA and Sidak post test). To determine whether SEC-based EV purification affects the profile of eFat-EVs, we isolated (UC) and purified (SEC) EVs from the same medium samples and analyzed several representative cytokines by enzyme-linked immunosorbent assay. Cytokine analysis revealed that unpurified (UC), and particularly purified (SEC) eFat-EVs from patients with AF carried a greater number of cytokines, such as IL1- $\alpha$  (**I**), adiponectin (**J**), osteopontin (**K**), and IL-6 (**L**). The amount of TNF- $\alpha$  was greater in unpurified eFat-EVs from patients with AF than patients without AF (**M**). The amounts of purified and unpurified EV-encapsulated cytokine IL1- $\beta$  (**N**) were similar in patients with and without AF, independent of the mode of EV separation ( $n=5$ , results are presented as the mean of cytokine levels per 50  $\mu\text{g}$  of protein  $\pm$  SEM,  $P$  values by Mann-Whitney  $U$  test). AF indicates atrial fibrillation; eFat, epicardial fat; EVs, extracellular vesicles; FSC, forward scatter; HDL, high-density lipoprotein; IL, interleukin; LDL, low-density lipoprotein; NTA, nanoparticle-tracking analysis; SEC, size exclusion chromatography; SSC, side scattered; TNF- $\alpha$ , tumor necrosis factor- $\alpha$ ; UC, ultracentrifugation; and VLDL, very low density lipoprotein.

### eFat-EVs Targeted ECs and Stimulated Angiogenesis

Recent evidence suggests that ECs have a role in the pathogenesis of atrial fibrosis and AF.<sup>34</sup> To determine whether eFat-EVs can target and affect ECs, we labeled eFat-EVs with the fluorescent dye PKH26 and incubated the labeled EVs with human umbilical cord vascular endothelial cells. We observed an intensive uptake

of EVs by the ECs that peaked within an hour and persisted for 56 hours (Figure 6A and 6B, and [Movie 1 in the Data Supplement](#)). Therefore, eFat-EVs effectively targeted human ECs. To determine the angiogenic impact of eFat-EVs, we used the angiogenic tube formation assay. Before purification (UC), eFat-EVs from patients with AF had a greater angiogenic capacity and increased the number of polygons by 300%, compared with patients without AF (Figure 6C and 6D). After SEC-based

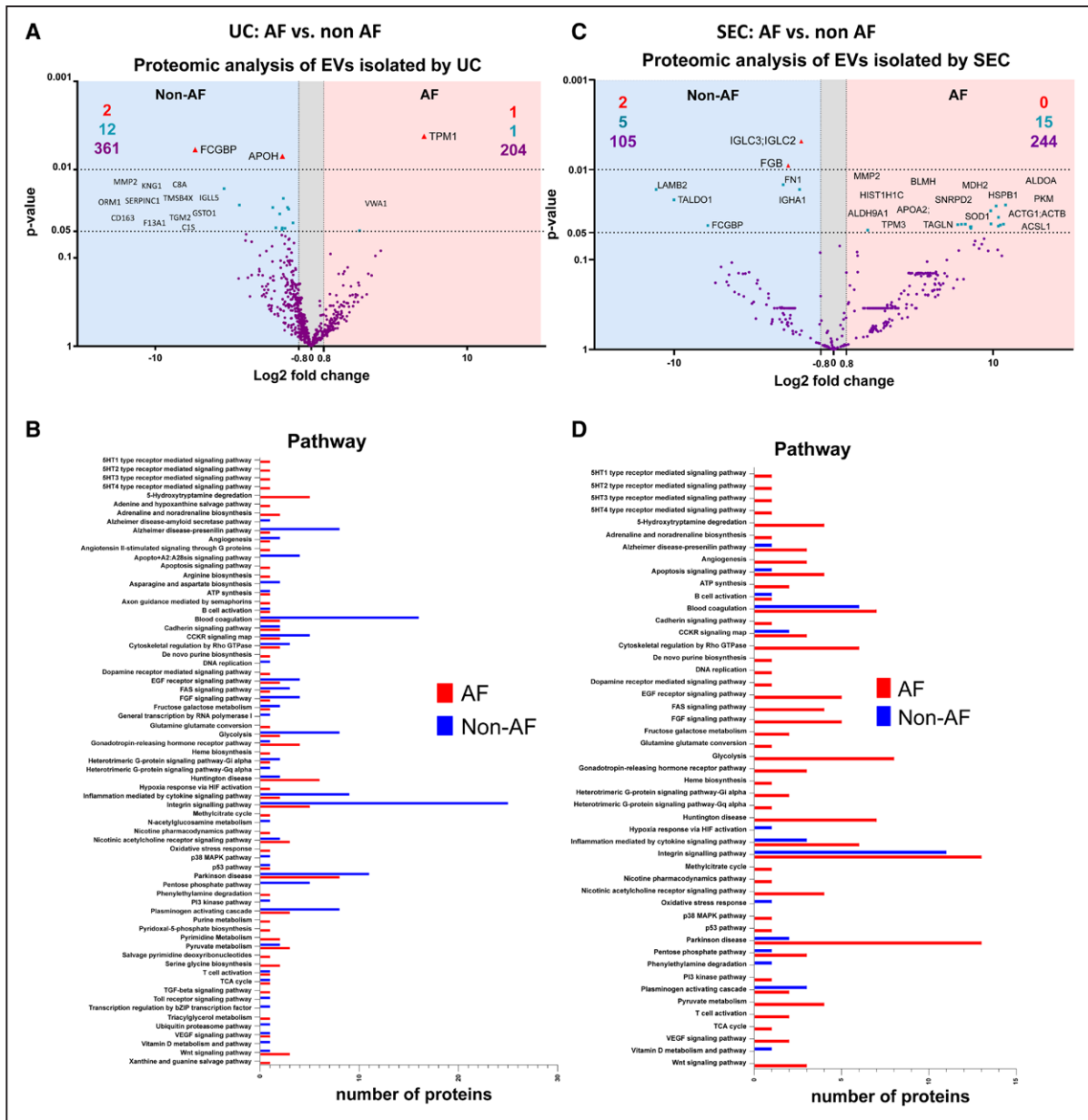


**Figure 4. Proteomic profiling of eFat-EVs.**

To determine differences in the proteome of crude and purified eFat-EVs from patients with and without AF, we performed a comparative proteomic analysis. First, we compared the proteome of unpurified eFat-EVs (isolated by UC), from patients with vs without AF. **A**, To graphically present the quantitative data, we constructed a volcano of plot ( $\log_2$  fold change of AF vs non-AF) vs  $P$  value. Volcano plot illustrates significantly differentially abundant proteins in unpurified eFat-EVs from patients with and without AF. Points above the lower nonaxial horizontal line represent proteins with significantly different abundances ( $P < 0.05$ ). Points to the left of the left-most nonaxial vertical line denote protein  $\log_2$  fold changes of AF/non-AF that are lower than  $-0.8$ , whereas points to the right of the right-most nonaxial vertical line denote protein fold changes of AF/non-AF  $> 0.8$ . Colored numbers at the right and left upper corners indicate: red,  $P < 0.01$ ; blue,  $0.01 < P < 0.05$ ; purple,  $P > 0.05$ . **B**, PANTHER classification of unpurified (UC) eFat-EV protein categories: AF vs non-AF. Unpurified eFat-EV-derived proteins were clustered according to different categories by the PANTHER classification system (<http://pantherdb.org>). Analysis of biological pathways revealed that pathways relevant to fibrosis, angiogenesis, and coagulation were present in EVs from patients with and without AF, with more abundance in EVs from patients without AF. PANTHER pathway classification related to fibrosis and hypertrophy such as transforming growth factor- $\beta$  and 5-hydroxytryptamine pathways were exclusively expressed in eFat-EVs from patients with AF. Next, we analyzed the proteome of purified eFat-EVs (isolated by SEC), from patients with vs without AF. **C**, Volcano plot illustrates significantly differentially abundant proteins in pure eFat-EVs from patients with vs without AF. **D**, PANTHER classification of purified (SEC) eFat-EV protein categories: AF vs non-AF. Purified eFat-EV-derived proteins were clustered according to different categories by the PANTHER classification system. PANTHER pathway classification revealed that pathways related to atrial fibrosis, angiogenesis, apoptosis, and myopathy are exclusively expressed in purified eFat-EVs from patients with AF (including wingless and Int-1 pathway signaling, 5-hydroxytryptamine pathways, T-cell activation, VEGF, FGF, and EGF signaling). AF indicates atrial fibrillation; eFat, epicardial Fat; EGF, epidermal growth factor; EVs, extracellular vesicles; FGF, fibroblast growth factor; PANTHER, (Protein Analysis Through Evolutionary Relationships; SEC, size exclusion chromatography; VEGF, vascular endothelial growth factor; TCA cycle, tricarboxylic acid cycle; TGF, transforming growth factor; UC, ultracentrifugation; and VEGF, vascular endothelial growth factor.

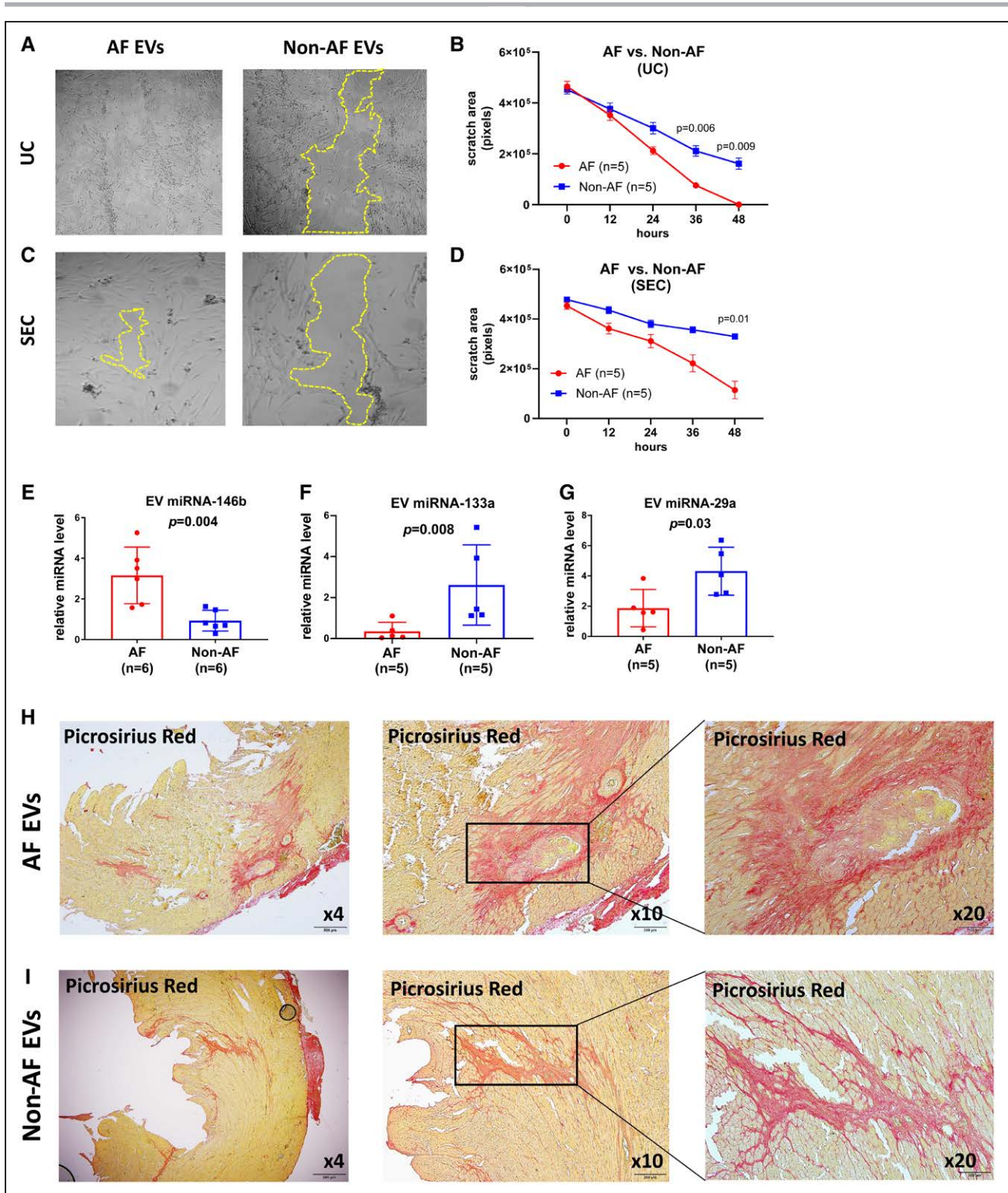


**Figure 5. eFat-EVs stimulated fibrosis.**

To determine whether eFat-EVs stimulate cardiac fibrosis, we used human MSCs from the right atrial appendage and migration scratch assay. We scratched the sheet of cultured MSCs with the tip of pipette (10  $\mu$ L). Next, we exposed the MSCs to eFat-EVs (50  $\mu$ g/mL of protein) from patients with and without AF. **A**, Representative images of human MSCs, 48 hours after scratch and exposure to unpurified eFat-EVs from patients with and without AF. **B**, Unpurified eFat-EVs from patients with AF had a greater effect on MSC proliferation, migration, and gap closure than those from patients without AF (n=5, data shown as scratch area in pixels, *P* values calculated by repeated-measures 2-way ANOVA and Sidak post test). **C**, To exclude the effect of contaminated proteins, we repeated the scratch assay using SEC-based purified eFat-EVs. Representative images of human MSCs, 48 hours after scratch and exposure to purified eFat-EVs from patients with and without AF. **D**, Purified eFat-EVs from patients with AF had a greater effect on MSC proliferation, migration, and gap closure, than those from (Continued)

**Figure 5 Continued.** patients without AF (n=5, data shown as scratch area in pixels, *P* values calculated by repeated-measures 2-way ANOVA and Sidak post test). **E** through **G**, To determine the potential role of eFat-EV–derived miRNA, we used polymerase chain reaction to assess specific EV-encapsulated miRNAs that could influence cardiac fibrosis. The expression of profibrotic EV-encapsulated miR-146b was higher (**E**), whereas antifibrotic miR-133 (**F**) and miR-29a (**G**) were lower in eFat-EVs from patients with AF, than those without AF (n=5, data shown as relative miRNA expression level, calculated values were normalized to U6, *P* values by Mann-Whitney *U* test). **H** and **I**, To confirm profibrotic properties of eFat-EVs in vivo, we injected eFat-EVs from patients with and without AF to the left ventricular free wall of Sprague-Dawley female rats (250–300 g; n=3). Picrosirius-Red staining for collagen revealed extensive myocardial fibrosis in the hearts treated with eFat-EVs from patients with AF. The extent of fibrosis appeared smaller in hearts treated with eFat-EVs from patients without AF (**I**). AF indicates atrial fibrillation; eFat, epicardial fat; EVs, extracellular vesicles; MSCs, mesenchymal stromal cells; SEC, size exclusion chromatography; and UC, ultracentrifugation.

purification, eFat-EVs from patients with AF increased the number of polygons by 100% (Figure 6E and 6F). Although our data confirmed the independent biological effect of eFat-EVs, the number of polygons was decreased by >50%, after treatment with purified EVs (SEC), compared with unpurified EVs (UC). This change was likely attributable to the elimination of contaminated proangiogenic proteins. Overall, our results indicated that eFat-EVs are efficiently transported into human ECs and stimulate angiogenesis.

### Proarrhythmic Properties of eFat-EVs

Although it is likely that eFat-EVs contribute to the formation of the arrhythmogenic substrate by way of inflammation and fibrosis, it is possible that there is a direct effect on atrial electrophysiology. To study the causal association of the eFat-EVs on the electrophysiological properties of human cardiomyocytes, we used a novel 2-dimensional hiPSC-based cardiomyocyte tissue model.<sup>20</sup> We generated hiPSC-derived cardiac cell sheets (hiPSC-CCSs) that stably express the genetically encoded voltage fluorescent indicator ArcLight.<sup>20</sup> The engineered cells enable long-term repeated functional assessment of the same hiPSC-CCS tissue over time by using optical mapping.

From the optically derived action potentials we were able to construct detailed activation and repolarization maps, enabling the measurements of multiple electrophysiological parameters. For the electrophysiological experiments, we purified eFat-EVs by a sucrose (30%) cushion. We found that the sucrose cushion eliminated the contaminated endoplasmic reticulum as indicated by the resident protein calreticulin (Figure V in the Data Supplement).

Next, we incubated the purified eFat-EVs with the hiPSC-CCSs. We found that eFat-EVs from patients with and without AF shortened the APD<sub>80</sub>, after 168 hours of exposure, compared with phosphate-buffered saline (Figure 7A). This is important because shortening of the APD predisposes cardiomyocytes to AF and is the hallmark of electrophysiological remodeling in AF. eFat-EVs from patients with and without AF did not affect the conduction velocity, after 168 hours of exposure, compared with phosphate-buffered saline (Figure 7B).

Optical mapping provides high resolution of rotors, reentrant spiral waves that can generate fibrillatory atrial

activity in AF, and important insights into the pathogenesis and mechanisms of AF. After 168 hours of exposure to eFat-EVs, we evaluated potential differences in reentrant arrhythmia (rotor) propensity between the different groups using pacing protocols. We induced sustained rotor in 3 of the 6 hiPSC-CCSs treated with eFat-EVs from patients with AF (3 of 6 versus 0 of 15, *P*=0.01; Figure 7C and 7E). The induced rotors in this group were sustained (lasting minutes and even hours) and could not be electrically cardioverted (Figure 7C and 7E and Movie II in the Data Supplement). In contrast, we were unable to induce stable rotors in hiPSC-CCSs treated with eFat-EVs from patients without AF or phosphate-buffered saline (Figure 7D, 7F, and 7G). In each control group, we were able to induce transient reentrant arrhythmias in a single culture. Moreover, the duration of induced reentrant activity was brief, and self-terminated 2 to 3 seconds after initiation. Together, the optical mapping experiments indicated that eFat-EVs from patients with AF promote the initiation and maintenance of reentrant arrhythmias in the hiPSC-CCS tissue model.

### DISCUSSION

The present study is the first to examine the role of eFat-EVs in the pathogenesis of AF. Our work reveals a previously unrecognized pathway involved in the development of atrial myopathy and AF. eFat of patients with AF secretes a high amount of EVs that harbor a unique proinflammatory, profibrotic, and proarrhythmic signature. Here, we provide evidence that eFat-EVs stimulate inflammation, fibrosis, and reentry, all of which can trigger and sustain AF (Figure 8). Thus, our findings add to emerging insights on the role of eFat in the pathogenesis of AF.<sup>8–10</sup>

### eFat-EVs Mediate Cellular and Electric Remodeling

Here we confirm and extend previous reports,<sup>8–10,12,13,35</sup> and show robust inflammation, fibrosis, angiogenesis, and apoptosis in the eFat tissues from patients referred for heart surgery. eFat can affect the adjacent myocardium by paracrine mechanisms, and by direct cell infiltration, as well.<sup>10–13</sup> Atrial inflammation and fibrosis are the hallmarks of this process,<sup>28</sup> and result in atrial myopathy and remodeling.<sup>10–12,36</sup> A new finding of interest was the

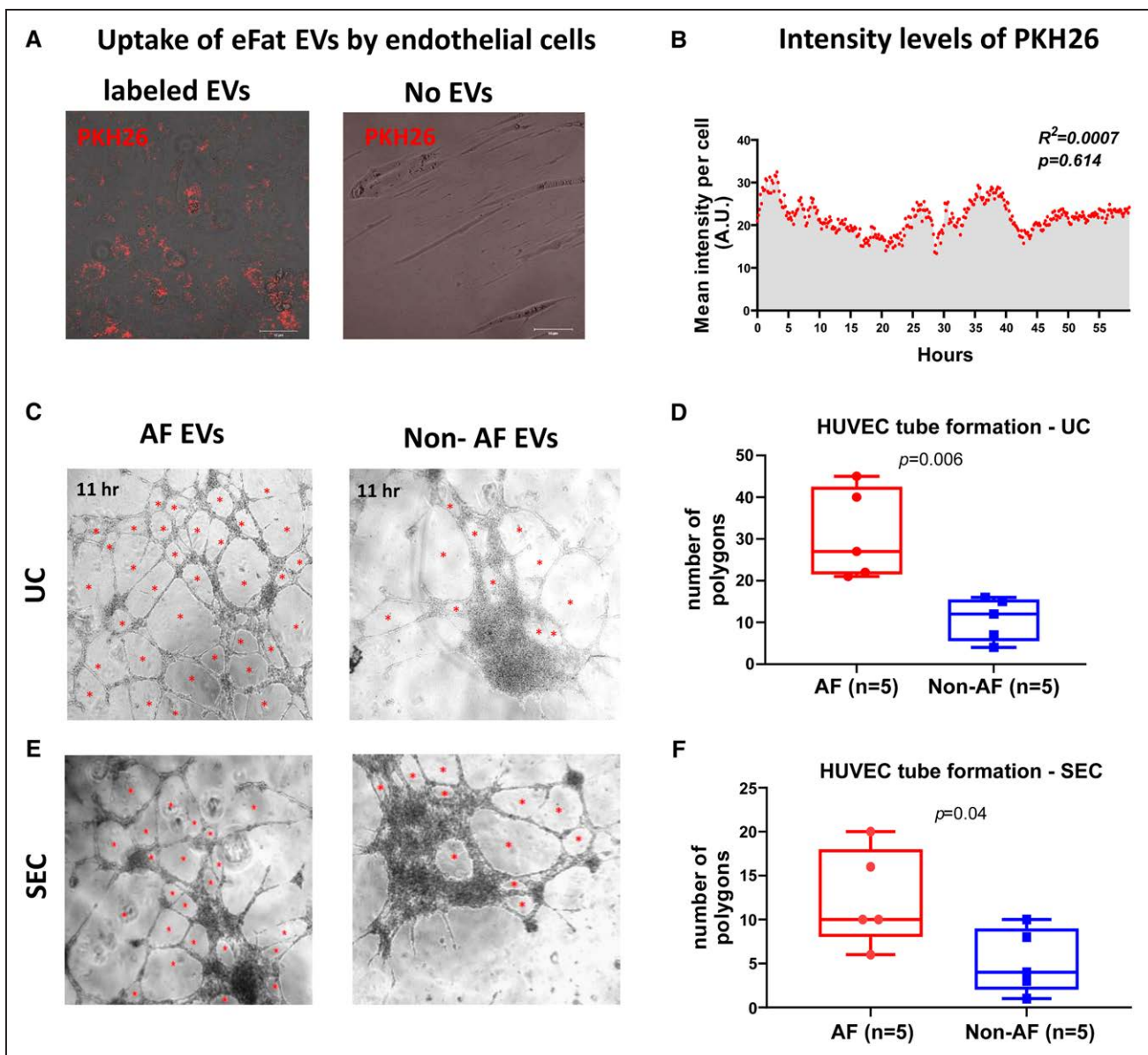


**Figure 6. eFat-EVs targeted endothelial cells and simulated angiogenesis.**

To determine whether eFat-EVs can target endothelial cells, we labeled eFat-EVs with the PKH26 fluorescent dye and incubated them with HUVECs. **A**, Representative images of PKH26-labeled eFat-EVs uptake labeled with PKH26, by HUVEC cells after 11 hours ( $n=2$ ; scale bar, 50  $\mu\text{m}$ ). **B**, An intensive uptake of eFat-EVs by the ECs that peaked within 1 hour from incubation and remained stable for 56 hours. Data shown as mean intensity per cell,  $P$  value and  $R^2$  were calculated by simple linear regression. **C**, To evaluate the angiogenic power of eFat-EVs, we used the angiogenic tube formation assay. Representative images of angiogenic tube formation of HUVEC cells incubated with eFat-EVs from patients with and without AF after 11 hours ( $n=5$ ; scale bar, 200  $\mu\text{m}$ ). **D**, Unpurified eFat-EVs from patients with AF had a greater angiogenic effect than patients without AF ( $n=5$ , data are shown as the number of polygons,  $P$  values were calculated by Mann-Whitney  $U$  test). **E**, To isolate the effect of protein contamination on the proangiogenic effects of eFat-EVs, we repeated the angiogenic tube formation assay after eFat-EVs purification by SEC. Representative images of angiogenic tube formation of HUVEC cells incubated with purified eFat-EVs from patients with and without AF after 11 h ( $n=5$ , scale bar, 200  $\mu\text{m}$ ). **F**, After SEC-based purification, the angiogenic effect of eFat-EVs was preserved. eFat-EVs from patients with AF had a greater angiogenic effect than those from patients without AF ( $n=5$ , data shown as number of polygons,  $P$  values were calculated by Mann-Whitney  $U$  test). AF indicates atrial fibrillation; eFat, epicardial Fat; EVs, extracellular vesicles; HUVEC, human umbilical vein endothelial cells; PKH26, red fluorescent cell linker kits for general cell membrane labeling; SEC, size exclusion chromatography; and UC, ultracentrifugation.

robust expression of angiotensin-converting enzyme 2 in the fresh eFat tissues. Angiotensin-converting enzyme 2 mediates the entry of SARS-CoV-2 into cells. This finding may explain the vulnerability of obese patients to COVID-19<sup>21</sup> and associated cardiac complications.<sup>37</sup>

eFat-EVs can promote atrial fibrosis that forms the arrhythmogenic substrate for AF. Atrial fibrosis disrupts conduction between cardiomyocytes and generate regions of local conduction block and conduction heterogeneities, thereby favoring reentry and perpetuation

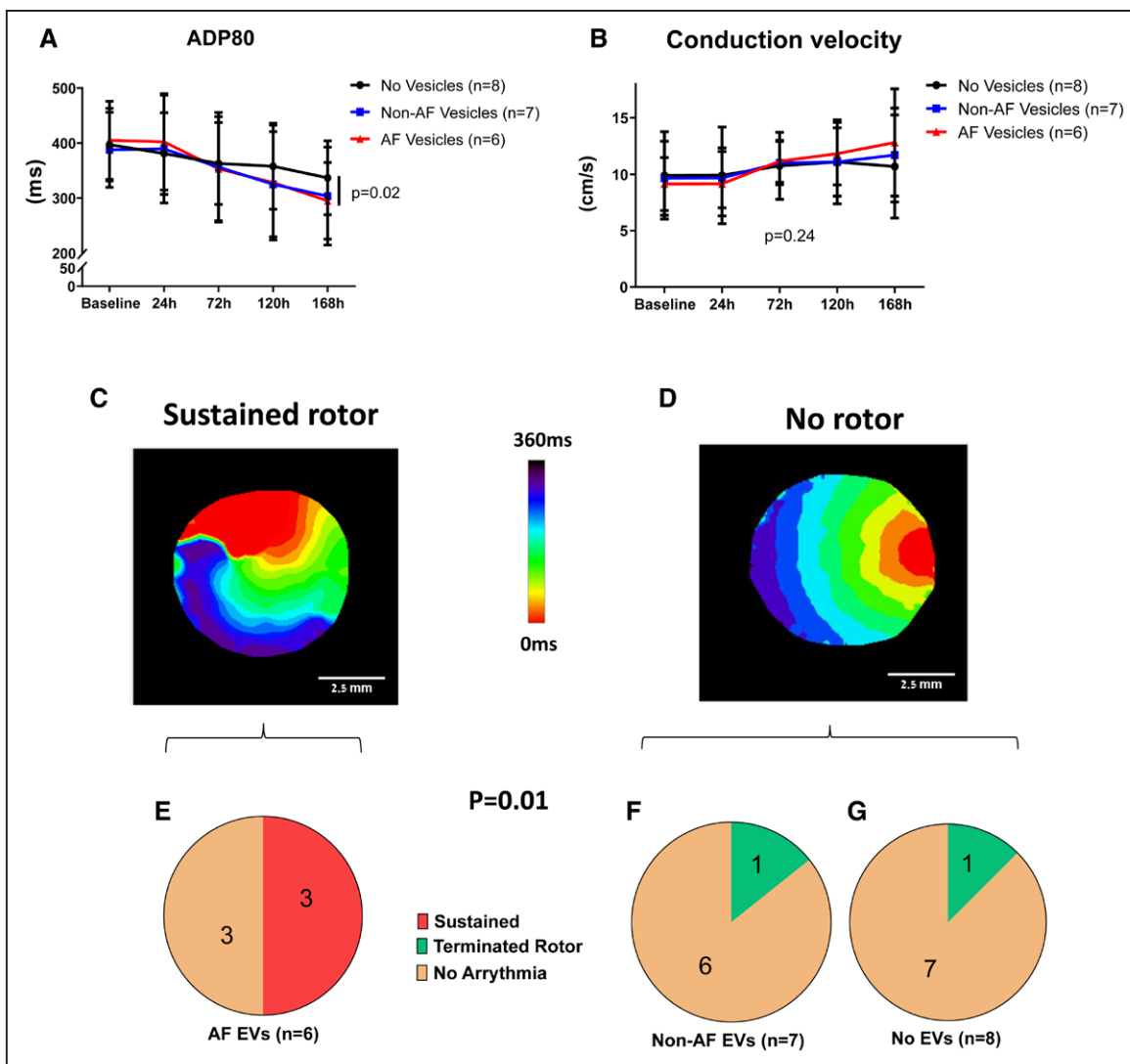


**Figure 7. eFat-EVs modify hiPSC-CCSs' electrophysiological properties and facilitate reentry.**

To study the potential effects of the EVs on the electrophysiological properties of human cardiac tissue, we generated hiPSC-derived cardiac cell sheets (hiPSC-CCSs) that express the genetically encoded voltage fluorescent indicator ArcLight. We used a high-density 30% sucrose cushion to eliminate microsomes and apoptotic bodies from eFat-EVs, and incubated purified eFat-EVs or phosphate-buffered saline (no vesicles) with hiPSC-CCSs. **A**, EVs derived from patients with and without AF shortened the  $APD_{80}$  (action potential duration at 80% of repolarization) after 120 and 168 hours of eFat-EV exposure compared with phosphate-buffered saline. A linear mixed-effects model showed a significant decrease in  $APD_{80}$  over time ( $P<0.0001$ ). Over time, the pattern differed significantly by treatment ( $P$  for treatment by time interaction=0.0006). The slope of  $APD_{80}$  change over time (estimate $\pm$ SE) with non-AF vesicles, control vesicles, and AF vesicles was  $-9.3\pm 1.2$ ,  $-13.1\pm 1.2$ , and  $-16.1\pm 1.3$  (ms/24 h), respectively ( $P=0.003$  for the AF vesicle s no vesicles;  $P=0.1$  for control vesicles vs no vesicles). At the 169-hour time point, the mean shortening in  $APD_{80}$  from baseline was  $49.6\pm 19.1$  ms higher in the AF vesicles compared with no vesicles ( $P=0.02$ ). **B**, The change in conduction velocity over time was similar in the 3 groups ( $P=0.24$ ). **C** and **D**, Representative images of activation maps derived after programmed electric stimulation show sustained rotor activity (**C**) and normal activation (**D**) of hiPSC-CCSs after treatment with eFat-EVs from patients with and without AF. **E** through **G**, Pie charts show the percentage of sustained rotor generation, nonsustained (transient) rotor generation, and no arrhythmia after treatment with eFat-EVs from patients with AF (**E**) or without AF (**F**) or without EVs (**G**). Note the significant increase in the inducibility of sustained rotor in the group of hiPSC-CCSs, treated with eFat-EVs from patients with AF, compared with the merged group hiPSC-CCSs, treated with eFat-EVs from patients without AF or phosphate-buffered saline (3 of 6 vs 0 of 15,  $P=0.01$  by Fisher exact test). ADP indicates action potential duration; AF, atrial fibrillation; CCSs, cardiac cell sheets; eFat, epicardial fat; EVs, extracellular vesicles; and hiPSC, human induced pluripotent stem cells.

of arrhythmias.<sup>38</sup> Moreover, mediators of inflammation and fibrosis can directly modify atrial electrophysiology, thereby leading to increased susceptibility to AF.<sup>39,40</sup> For example, inflammation and fibrosis modulates calcium homeostasis and connexins, which are associated with

triggers of AF and slow atrial conduction.<sup>13,29,39,41</sup> Here we show that eFat-EVs shorten APD in cardiomyocytes. APD shortening in atrial tissue has been described in animal models of obesity and AF.<sup>42,43</sup> Obesity is associated with a shortened effective refractory period in the pulmonary

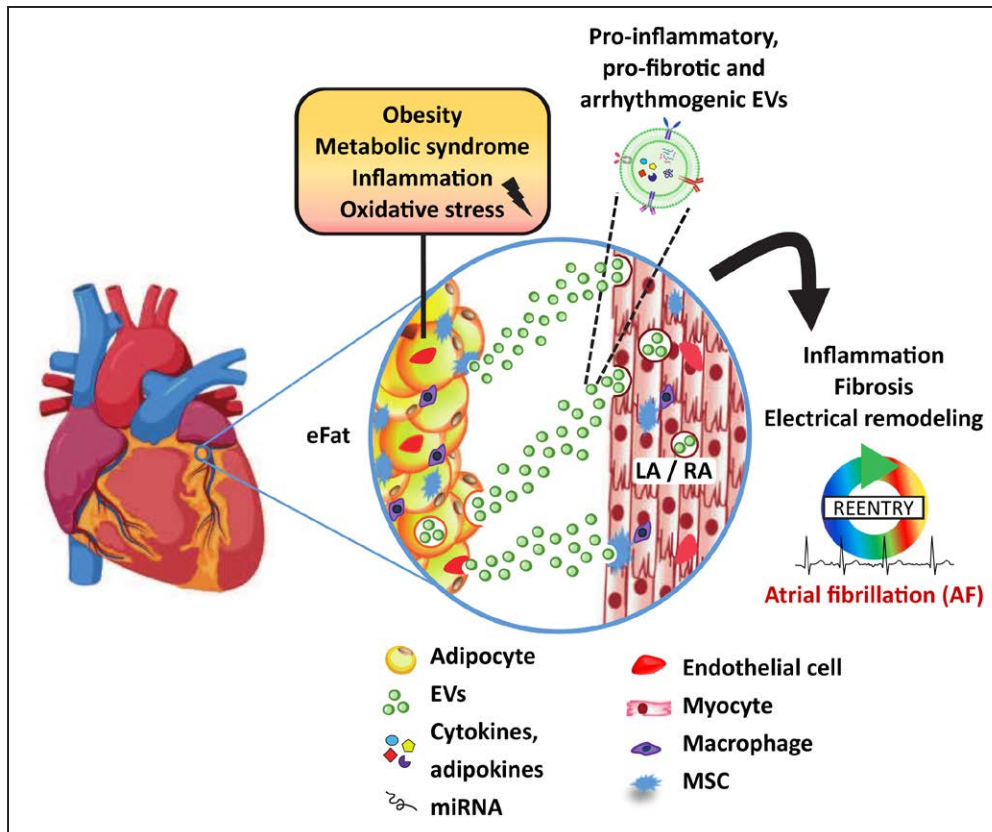


**Figure 8. eFat-EVs trigger atrial inflammation, fibrosis, and fibrillation.**

Systemic disorders such as metabolic syndrome, obesity, and oxidative stress stimulate eFat expansion, inflammation, and fibrosis. EVs secreted from eFat carry proinflammatory, profibrotic, and proarrhythmic molecules. eFat-EVs target atrial cells such as cardiomyocytes, mesenchymal stromal cells, and endothelial cells. eFat-EVs induce cellular, molecular, and electrophysiological remodeling resulting in atrial myopathy and generation of the arrhythmogenic substrate for the initiation and maintenance of AF. AF indicates atrial fibrillation; eFat, epicardial fat; EVs, extracellular vesicles; LA, left atrium; MSC, mesenchymal stromal cells; and RA, right atrium. Created with BioRender.com.

veins, leading to the notion that adiposity can predispose to the initiation of AF.<sup>44</sup> A shortened effective refractory period is also the main electrophysiological parameter that is affected in the process of AF-induced atrial remodeling.<sup>45</sup> The mechanism of obesity-induced APD shortening, however, is not entirely clear. eFat secretes cytokines that directly influence electric remodeling.<sup>11,12,46</sup> Inflammatory cytokines such as TNF- $\alpha$ , IL-1, and IL-6, are arrhythmogenic by directly modulating the function of cardiac ion channels.<sup>24</sup> Here we show that eFat-EVs are rich in TNF- $\alpha$ , IL-1, and IL-6 and predispose induced pluripotent stem cell-derived cardiomyocytes to reentrant arrhythmias. Together, eFat-EVs can induce both structural and electric remodeling that promotes an AF-prone milieu.

### Methods of EV Isolation Face Significant Limitations

EV studies are limited by the imperfections of EV isolation methods.<sup>15,18</sup> The assessment of EV biological activities is difficult because there is no gold standard protocol for complete recovery of EVs with their native shape and function.<sup>15,18</sup> A major obstacle in EV isolation and separation is protein contamination.<sup>18</sup> Here, we tested several methods to isolate and purify eFat-EVs, namely,

comparing UC with SEC. The latter emerged as a reliable, efficient, and reproducible method to improve EV recovery, eliminate protein contamination, preserve vesicle structure, and maintain biological activity of EVs.<sup>25</sup> Purification and enrichment of EVs, however, may attenuate the biological impact of unpurified EVs. This reduced effect was most likely attributable to removal of contaminated proteins, which also play a causal role in the pathogenesis of atrial myopathy and fibrillation in vivo.

Another obstacle was ensuring that recovered vesicles were truly from the extracellular space, rather than being intracellular vesicles or artefactual particles released from damaged cells or tissues.<sup>18</sup> Here, to ensure that the EVs were not artefactually created from damaged cells, we cultured the eFat tissue for 9 days.<sup>47</sup> The rationale for a 9-day organ culture was based on a previous work that showed that at the early days of culture (1–2 days), the levels of inflammatory cytokine were high, compared with the levels in freshly obtained adipose tissue.<sup>47</sup> Thus, short-term incubation would not have been appropriate for our work. Last, previous reports have suggested that organ culture is the preferred method to assess the long-term regulation of gene expression and adipocyte function within the adipose tissue, and the correlation with in vivo effects, as well.<sup>48</sup>

Last, apoptotic cells and bodies may contaminate EVs isolated from cells.<sup>49</sup> In our work, we used several approaches to exclude apoptotic body contamination. We found that high-density sucrose cushion eliminated the endoplasmic reticulum

contamination, as indicated by the resident protein calreticulin. But apoptosis characterizes pathological fat deposition because the abnormal expansion of adipose tissue generates areas of inflammation, fibrosis, and hypoxia, leading to cell necrosis and apoptosis.<sup>50</sup> We observed many apoptotic cells in fresh eFat specimens from cardiac patients with and without AF. Thus, our culture conditions captured the situation in vivo.

## Summary, Potential Implications, and Future Research

This study is the first to suggest that eFat-EVs contribute, at least in part, to the development of atrial myopathy and AF (Figure 8). We show that dissemination of the eFat signals through EVs can impact human cardiac cells and increase vulnerability to reentry. These new findings may also shed light on the pathogenesis of other cardiovascular diseases linked to eFat and obesity, such as coronary artery disease, cardiac ageing, and heart failure with preserved ejection fraction. However, further research is needed to confirm this relation to these other diseases. Another challenge will be to translate our results into clinical application in terms of EV-based diagnostics and therapies to modify eFat inflammation and fibrosis. The relationship between eFat and AF is multifactorial and bidirectional. Understanding of the eFat physiology and the relative role of EVs may help us to improve future therapies to prevent and treat AF and possibly other cardiovascular diseases.

## ARTICLE INFORMATION

Received October 11, 2020; accepted March 9, 2021.

### Affiliations

Neufeld and Tamman Cardiovascular Research Institutes (O.S.-T., R.Y.B., N.N.-S., N.L., Y.S., L.-P.L.-K., J.L.), Department of Cardiac Surgery, Leviev Cardiothoracic and Vascular Center (E. Ram, E.M.Z., S.A., L.S., E. Raanani), Sheba Medical Center, Sackler School of Medicine, Tel Aviv University, Israel. Heart Center, Sheba Medical Center, Tel Hashomer, Israel (O.S.-T., E. Ram, R.Y.B., N.N.-S., N.L., Y.S., L.-P.L.-K., D.V., E.M.Z., S.A., L.S., E. Raanani, J.L.). The Sohnis Family Laboratory for Cardiac Electrophysiology and Regenerative Medicine, Rappaport Faculty of Medicine, Technion Institute of Technology, Israel (N.B., L.G.). Cancer Research Center, Chaim Sheba Medical Center, Tel Hashomer, Israel (R.M.). Smoler Proteomics Center, Faculty of Biology, Technion-Israel Institute of Technology, Haifa, Israel (T.Z.). Department of Biomolecular Sciences, Weizmann Institute of Science, Rehovot, Israel (N.R.-R.).

### Acknowledgments

We thank N. Ziv-Crispel and V. York for skillful English-language editing. We thank Dr Théry for helpful advice on the methods to isolate and purify EVs. We thank Dr Aronson for helpful statistical advice. Proteomic analysis was done by the Smoler Proteomics Center at the Technion (Haifa, Israel). This work was performed in partial fulfillment of requirements for the PhD degree of O. Shaihov-Teper, Sackler Faculty of Medicine, Tel Aviv University, Israel.

### Sources of Funding

Support for this project was provided by a grant from the Seymour Feffer Foundation and the Israel Science Foundation (ISF). This study was partially funded by the European Research Council (ERC-2017-COG-773181-iPS-ChOp-AF).

### Disclosures

None.

## Supplemental Materials

Expanded Methods  
Data Supplement Figures I–V  
Data Supplement Tables I and II  
References 51–62  
Movies I and II

## REFERENCES

- Patel NJ, Deshmukh A, Pant S, Singh V, Patel N, Arora S, Shah N, Chothani A, Savani GT, Mehta K, et al. Contemporary trends of hospitalization for atrial fibrillation in the United States, 2000 through 2010: implications for healthcare planning. *Circulation*. 2014;129:2371–2379. doi: 10.1161/CIRCULATIONAHA.114.008201
- Chung MK, Refaat M, Shen WK, Kutyla V, Cha YM, Di Biase L, Baranchuk A, Lampert R, Natale A, Fisher J, et al; ACC Electrophysiology Section Leadership Council. Atrial fibrillation: JACC council perspectives. *J Am Coll Cardiol*. 2020;75:1689–1713. doi: 10.1016/j.jacc.2020.02.025
- Kornej J, Börschel CS, Benjamin EJ, Schnabel RB. Epidemiology of atrial fibrillation in the 21st century: novel methods and new insights. *Circ Res*. 2020;127:4–20. doi: 10.1161/CIRCRESAHA.120.316340
- Goette A, Kalman JM, Aguinaga L, Akar J, Cabrera JA, Chen SA, Chugh SS, Corradi D, D'Avila A, Dobrev D, et al. EHRA/HRS/APHRS/SOLAECE expert consensus on atrial cardiomyopathies: definition, characterization, and clinical implication. *Heart Rhythm*. 2017;14:e3–e40. doi: 10.1016/j.hrthm.2016.05.028
- Goldberger JJ, Arora R, Green D, Greenland P, Lee DC, Lloyd-Jones DM, Markl M, Ng J, Shah SJ. Evaluating the atrial myopathy underlying atrial fibrillation: identifying the arrhythmogenic and thrombogenic substrate. *Circulation*. 2015;132:278–291. doi: 10.1161/CIRCULATIONAHA.115.016795
- Shen MJ, Arora R, Jalife J. Atrial myopathy. *JACC Basic Transl Sci*. 2019;4:640–654. doi: 10.1016/j.jaccbts.2019.05.005
- Magnussen C, Niiranen TJ, Ojeda FM, Gianfagna F, Blankenberg S, Njølstad I, Vartiainen E, Sans S, Pasterkamp G, Hughes M, et al; BiomarcARE Consortium. Sex differences and similarities in atrial fibrillation epidemiology, risk factors, and mortality in community cohorts: results from the BiomarcARE Consortium (Biomarker for Cardiovascular Risk Assessment in Europe). *Circulation*. 2017;136:1588–1597. doi: 10.1161/CIRCULATIONAHA.117.028981
- Bos D, Vernooij MW, Shahzad R, Kavousi M, Hofman A, van Walsum T, Deckers JW, Ikram MA, Heeringa J, Franco OH, et al. Epicardial fat volume and the risk of atrial fibrillation in the general population free of cardiovascular disease. *JACC Cardiovasc Imaging*. 2017;10:1405–1407. doi: 10.1016/j.jcmg.2016.12.005
- Wong CX, Ganesan AN, Selvanayagam JB. Epicardial fat and atrial fibrillation: current evidence, potential mechanisms, clinical implications, and future directions. *Eur Heart J*. 2017;38:1294–1302. doi: 10.1093/eurheartj/ehw045
- Packer M. Epicardial adipose tissue may mediate deleterious effects of obesity and inflammation on the myocardium. *J Am Coll Cardiol*. 2018;71:2360–2372. doi: 10.1016/j.jacc.2018.03.509
- Mazurek T, Zhang L, Zalewski A, Mannion JD, Diehl JT, Arafat H, Sarov-Blat L, O'Brien S, Keiper EA, Johnson AG, et al. Human epicardial adipose tissue is a source of inflammatory mediators. *Circulation*. 2003;108:2460–2466. doi: 10.1161/01.CIR.0000099542.57313.C5
- Venteclef N, Guglielmi V, Balse E, Gaborit B, Cottillard A, Atassi F, Amour J, Leprince P, Dutour A, Clément K, et al. Human epicardial adipose tissue induces fibrosis of the atrial myocardium through the secretion of adipofibrokines. *Eur Heart J*. 2015;36:795–805a. doi: 10.1093/eurheartj/ehu099
- Nalliah CJ, Bell JR, Raaijmakers AJA, Waddell HM, Wells SP, Bernasocchi GB, Montgomery MK, Binny S, Watts T, Joshi SB, et al. Epicardial adipose tissue accumulation confers atrial conduction abnormality. *J Am Coll Cardiol*. 2020;76:1197–1211. doi: 10.1016/j.jacc.2020.07.017
- Shah R, Patel T, Freedman JE. Circulating extracellular vesicles in human disease. *N Engl J Med*. 2018;379:958–966. doi: 10.1056/NEJMra1704286
- Sluijter JPG, Davidson SM, Boulanger CM, Buzás EI, de Kleijn DPV, Engel FB, Giricz Z, Hausenloy DJ, Kishore R, Lecour S, et al. Extracellular vesicles in diagnostics and therapy of the ischaemic heart: position paper from the Working Group on Cellular Biology of the Heart of the European Society of Cardiology. *Cardiovasc Res*. 2018;114:19–34. doi: 10.1093/cvr/cvx211

16. Kita S, Maeda N, Shimomura I. Interorgan communication by exosomes, adipose tissue, and adiponectin in metabolic syndrome. *J Clin Invest*. 2019;129:4041–4049. doi: 10.1172/JCI129193
17. January CT, Wann LS, Alpert JS, Calkins H, Cigarroa JE, Cleveland JC Jr, Conti JB, Ellinor PT, Ezekowitz MD, Field ME, et al; ACC/AHA Task Force Members. 2014 AHA/ACC/HRS guideline for the management of patients with atrial fibrillation: executive summary: a report of the American College of Cardiology/American Heart Association Task Force on Practice Guidelines and the Heart Rhythm Society. *Circulation*. 2014;130:2071–2104. doi: 10.1161/CIR.0000000000000040
18. Théry C, Witwer KW, Aikawa E, Alcaraz MJ, Anderson JD, Andriantsitohaina R, Antoniou A, Arab T, Archer F, Atkin-Smith GK, et al. Minimal information for studies of extracellular vesicles 2018 (MISEV2018): a position statement of the International Society for Extracellular Vesicles and update of the MISEV2014 guidelines. *J Extracell Vesicles*. 2018;7:1535750. doi: 10.1080/20013078.2018.1535750
19. Kravtsova-Ivantsiv Y, Shomer I, Cohen-Kaplan V, Snijder B, Superti-Furga G, Gonen H, Sommer T, Ziv T, Admon A, Naroditsky I, et al. KPC1-mediated ubiquitination and proteasomal processing of NF- $\kappa$ B p105 to p50 restricts tumor growth. *Cell*. 2015;161:333–347. doi: 10.1016/j.cell.2015.03.001
20. Shaheen N, Shiti A, Huber I, Shinnawi R, Arbel G, Gepstein A, Setter N, Goldfracht I, Gruber A, Chorna SV, et al. Human induced pluripotent stem cell-derived cardiac cell sheets expressing genetically encoded voltage indicator for pharmacological and arrhythmia studies. *Stem Cell Reports*. 2018;10:1879–1894. doi: 10.1016/j.stemcr.2018.04.006
21. Malavazos AE, Goldberger JJ, Iacobellis G. Does epicardial fat contribute to COVID-19 myocardial inflammation? *Eur Heart J*. 2020;41:2333. doi: 10.1093/eurheartj/ehaa471
22. Raposo G, Stahl PD. Extracellular vesicles: a new communication paradigm? *Nat Rev Mol Cell Biol*. 2019;20:509–510. doi: 10.1038/s41580-019-0158-7
23. Furi I, Momen-Heravi F, Szabo G. Extracellular vesicle isolation: present and future. *Ann Transl Med*. 2017;5:263. doi: 10.21037/atm.2017.03.95
24. Lazzarini PE, Laghi-Pasini F, Boutjdir M, Capecchi PL. Cardioimmunology of arrhythmias: the role of autoimmune and inflammatory cardiac channelopathies. *Nat Rev Immunol*. 2019;19:63–64. doi: 10.1038/s41577-018-0098-z
25. Monguió-Tortajada M, Gálvez-Montón C, Bayes-Genis A, Roura S, Borràs FE. Extracellular vesicle isolation methods: rising impact of size-exclusion chromatography. *Cell Mol Life Sci*. 2019;76:2369–2382. doi: 10.1007/s00018-019-03071-y
26. Boing AN, van der Pol E, Grootemaat AE, Coumans FA, Sturk A, Nieuwland R. Single-step isolation of extracellular vesicles by size-exclusion chromatography. *J Extracell Vesicles*. Published online September 8, 2014. doi: 10.3402/jev.v3.23430
27. Sawaki D, Czibik G, Pini M, Ternacle J, Suffee N, Mercedes R, Marcellin G, Surenaud M, Marcos E, Gual P, et al. Visceral adipose tissue drives cardiac aging through modulation of fibroblast senescence by osteopontin production. *Circulation*. 2018;138:809–822. doi: 10.1161/CIRCULATIONAHA.117031358
28. Frustaci A, Chimenti C, Bellocci F, Morgante E, Russo MA, Maseri A. Histological substrate of atrial biopsies in patients with lone atrial fibrillation. *Circulation*. 1997;96:1180–1184. doi: 10.1161/01.cir.96.4.1180
29. Nattel S. Molecular and cellular mechanisms of atrial fibrillation in atrial fibrillation. *JACC Clin Electrophysiol*. 2017;3:425–435. doi: 10.1016/j.jacep.2017.03.002
30. Naftali-Shani N, Itzhaki-Alfia A, Landa-Rouben N, Kain D, Holbova R, Adutler-Lieber S, Molotski N, Asher E, Grupper A, et al. The origin of human mesenchymal stromal cells dictates their reparative properties. *J Am Heart Assoc*. 2013;2:e000253. doi: 10.1161/JAHA.113.000253
31. Thomou T, Mori MA, Dreyfuss JM, Konishi M, Sakaguchi M, Wolfrum C, Rao TN, Winnay JN, Garcia-Martin R, Grinspoon SK, et al. Corrigendum: adipose-derived circulating miRNAs regulate gene expression in other tissues. *Nature*. 2017;545:252. doi: 10.1038/nature22319
32. van den Berg NWE, Kawasaki M, Berger WR, Neefs J, Meulendijks E, Tijssen AJ, de Groot JR. MicroRNAs in atrial fibrillation: from expression signatures to functional implications. *Cardiovasc Drugs Ther*. 2017;31:345–365. doi: 10.1007/s10557-017-6736-z
33. Ranjan P, Kumari R, Verma SK. Cardiac fibroblasts and cardiac fibrosis: precise role of exosomes. *Front Cell Dev Biol*. 2019;7:318. doi: 10.3389/fcell.2019.00318
34. Kume O, Teshima Y, Abe I, Ikebe Y, Oniki T, Kondo H, Saito S, Fukui A, Yufu K, Miura M, et al. Role of atrial endothelial cells in the development of atrial fibrillation and fibrillation in response to pressure overload. *Cardiovasc Pathol*. 2017;27:18–25. doi: 10.1016/j.carpath.2016.12.001
35. Haemers P, Hamdi H, Guedj K, Suffee N, Farahmand P, Popovic N, Claus P, LePrince P, Nicoletti A, Jalife J, et al. Atrial fibrillation is associated with the fibrotic remodelling of adipose tissue in the subepicardium of human and sheep atria. *Eur Heart J*. 2017;38:53–61. doi: 10.1093/eurheartj/ehv625
36. Thomas L, Abhayaratna WP. Left atrial reverse remodeling: mechanisms, evaluation, and clinical significance. *JACC Cardiovasc Imaging*. 2017;10:65–77. doi: 10.1016/j.jcmg.2016.11.003
37. Lazzarini PE, Boutjdir M, Capecchi PL. COVID-19, arrhythmic risk, and inflammation: mind the gap! *Circulation*. 2020;142:7–9. doi: 10.1161/CIRCULATIONAHA.120.047293
38. Allesie MA, de Groot NM, Houben RP, Schotten U, Boersma E, Smeets JL, Crijns HJ. Electropathological substrate of long-standing persistent atrial fibrillation in patients with structural heart disease: longitudinal dissociation. *Circ Arrhythm Electrophysiol*. 2010;3:606–615. doi: 10.1161/CIRCEP.109.910125
39. Hu YF, Chen YJ, Lin YJ, Chen SA. Inflammation and the pathogenesis of atrial fibrillation. *Nat Rev Cardiol*. 2015;12:230–243. doi: 10.1038/nrcardio.2015.2
40. Li N, Brundel BJJM. Inflammation and proteostasis novel molecular mechanisms associated with atrial fibrillation. *Circ Res*. 2020;127:73–90. doi: 10.1161/CIRCRESAHA.119.316364
41. Igarashi T, Finet JE, Takeuchi A, Fujino Y, Strom M, Greener ID, Rosenbaum DS, Donahue JK. Connexin gene transfer preserves conduction velocity and prevents atrial fibrillation. *Circulation*. 2012;125:216–225. doi: 10.1161/CIRCULATIONAHA.111.053272
42. Martínez-Mateu L, Saiz J, Aromolaran AS. Differential modulation of  $I_{Kc}$  and  $I_{CaL}$  channels in high-fat diet-induced obese guinea pig atria. *Front Physiol*. 2019;10:1212. doi: 10.3389/fphys.2019.01212
43. Aromolaran AS, Colecraft HM, Boutjdir M. High-fat diet-dependent modulation of the delayed rectifier K<sup>+</sup> current in adult guinea pig atrial myocytes. *Biochem Biophys Res Commun*. 2016;474:554–559. doi: 10.1016/j.bbrc.2016.04.113
44. Munger TM, Dong YX, Masaki M, Oh JK, Mankad SV, Borlaug BA, Asirvatham SJ, Shen WK, Lee HC, Bielinski SJ, et al. Electrophysiological and hemodynamic characteristics associated with obesity in patients with atrial fibrillation. *J Am Coll Cardiol*. 2012;60:851–860. doi: 10.1016/j.jacc.2012.03.042
45. Wijffels MC, Kirchhof CJ, Dorland R, Allesie MA. Atrial fibrillation begets atrial fibrillation. A study in awake chronically instrumented goats. *Circulation*. 1995;92:1954–1968. doi: 10.1161/01.cir.92.7.1954
46. Lin YK, Chen YC, Chen JH, Chen SA, Chen YJ. Adipocytes modulate the electrophysiology of atrial myocytes: implications in obesity-induced atrial fibrillation. *Basic Res Cardiol*. 2012;107:293. doi: 10.1007/s00395-012-0293-1
47. Carswell KA, Lee MJ, Fried SK. Culture of isolated human adipocytes and isolated adipose tissue. *Methods Mol Biol*. 2012;806:203–214. doi: 10.1007/978-1-61779-367-7\_14
48. Fried SK, Moustaid-Moussa N. Culture of adipose tissue and isolated adipocytes. *Methods Mol Biol*. 2001;155:197–212. doi: 10.1385/1-59259-231-7:197
49. Jeppesen DK, Hvam ML, Primdahl-Bengtson B, Boysen AT, Whitehead B, Dyrskjøt L, Orntoft TF, Howard KA, Ostfeld MS. Comparative analysis of discrete exosome fractions obtained by differential centrifugation. *J Extracell Vesicles*. 2014;3:25011. doi: 10.3402/jev.v3.25011
50. Sun K, Kusminski CM, Scherer PE. Adipose tissue remodeling and obesity. *J Clin Invest*. 2011;121:2094–2101. doi: 10.1172/JCI45887
51. Consortium E-T, Hendrix A. EV-TRACK: transparent reporting and centralizing knowledge in extracellular vesicle research. *Nat Methods*. 2017;14:228–232. doi: 10.1038/nmeth.4185
52. Perez-Riverol Y, Csordas A, Bai J, Bernal-Llinares M, Hewapathirana S, Kundu DJ, Inuganti A, Griss J, Mayer G, Eisenacher M, et al. The PRIDE database and related tools and resources in 2019: improving support for quantification data. *Nucleic Acids Res*. 2019;47:D442–D450. doi: 10.1093/nar/gky1106
53. Monguió-Tortajada M, Roura S, Gálvez-Montón C, Pujal JM, Aran G, Sanjurjo L, Franquesa M, Sarrias MR, Bayes-Genis A, Borràs FE. Nanosized UCMSC-derived extracellular vesicles but not conditioned medium exclusively inhibit the inflammatory response of stimulated T cells: implications for nanomedicine. *Theranostics*. 2017;7:270–284. doi: 10.7150/thno.16154
54. Shu S, Yang Y, Allen CL, Hurley E, Tung KH, Minderman H, Wu Y, Ernstoff MS. Purity and yield of melanoma exosomes are dependent on isolation method. *J Extracell Vesicles*. 2020;9:1692401. doi: 10.1080/20013078.2019.1692401

55. Kesimer M, Scull M, Brighton B, DeMaria G, Burns K, O'Neal W, Pickles RJ, Sheehan JK. Characterization of exosome-like vesicles released from human tracheobronchial ciliated epithelium: a possible role in innate defense. *FASEB J*. 2009;23:1858–1868. doi: 10.1096/fj.08-119131
56. Naftali-Shani N, Levin-Kotler LP, Palevski D, Amit U, Kain D, Landa N, Hochhauser E, Leor J. Left ventricular dysfunction switches mesenchymal stromal cells toward an inflammatory phenotype and impairs their reparative properties via toll-like receptor-4. *Circulation*. 2017;135:2271–2287. doi: 10.1161/CIRCULATIONAHA.116.023527
57. Liang CC, Park AY, Guan JL. In vitro scratch assay: a convenient and inexpensive method for analysis of cell migration in vitro. *Nat Protoc*. 2007;2:329–333. doi: 10.1038/nprot.2007.30
58. Pužar Dominkuš P, Stenovec M, Sitar S, Lasič E, Zorec R, Plemenitaš A, Žagar E, Kreft M, Lenassi M. PKH26 labeling of extracellular vesicles: characterization and cellular internalization of contaminating PKH26 nanoparticles. *Biochim Biophys Acta Biomembr*. 2018;1860:1350–1361. doi: 10.1016/j.bbmem.2018.03.013
59. Schindelin J, Arganda-Carreras I, Frise E, Kaynig V, Longair M, Pietzsch T, Preibisch S, Rueden C, Saalfeld S, Schmid B, et al. Fiji: an open-source platform for biological-image analysis. *Nat Methods*. 2012;9:676–682. doi: 10.1038/nmeth.2019
60. Palevski D, Levin-Kotler LP, Kain D, Naftali-Shani N, Landa N, Ben-Mordechai T, Konfino T, Holbova R, Molotski N, Rosin-Arbesfeld R, et al. Loss of macrophage wnt secretion improves remodeling and function after myocardial infarction in mice. *J Am Heart Assoc*. 2017;6:e004387. doi: 10.1161/JAHA.116.004387
61. Shinnawi R, Huber I, Maizels L, Shaheen N, Gepstein A, Arbel G, Tijssen AJ, Gepstein L. Monitoring human-induced pluripotent stem cell-derived cardiomyocytes with genetically encoded calcium and voltage fluorescent reporters. *Stem Cell Reports*. 2015;5:582–596. doi: 10.1016/j.stemcr.2015.08.009
62. Huang X, Kim TY, Koren G, Choi BR, Qu Z. Spontaneous initiation of premature ventricular complexes and arrhythmias in type 2 long QT syndrome. *Am J Physiol Heart Circ Physiol*. 2016;311:H1470–H1484. doi: 10.1152/ajpheart.00500.2016